Annals of Botany **122**: 23–43, 2018
doi: 10.1093/aob/mcy043, available online at www.academic.oup.com/aob

ANNALS OF BOTANY
Founded 1887

Depletion of sucrose induces changes in the tip growth mechanism of tobacco pollen tubes

Luigi Parrotta[1,*], Claudia Faleri[1], Stefano Del Duca[2] and Giampiero Cai[1]

[1]Dipartimento Scienze della Vita, Università di Siena, via Mattioli 4, 53100 Siena, Italy and [2]Dipartimento Scienze Biologiche, Geologiche e Ambientali, Università di Bologna, via Irnerio 42, 40126 Bologna, Italy
**For correspondence. E-mail parrotta2@unisi.it*

Received: 3 January 2018 Returned for revision: 2 February 2018 Editorial decision: 7 March 2018 Accepted: 9 March 2018
Published electronically 12 April 2018

• **Background and Aims** Pollen tubes are rapidly growing, photosynthetically inactive cells that need high rates of energy to support growth. Energy can derive from internal and external storage sources. The lack of carbon sources can cause various problems during pollen tube growth, which in turn could affect the reproduction of plants.
• **Methods** We analysed the effects of energy deficiency on the development of *Nicotiana tabacum* pollen tubes by replacing sucrose with glycerol in the growth medium. We focused on cell growth and related processes, such as metabolite composition and cell wall synthesis.
• **Key Results** We found that the lack of sucrose affects pollen germination and pollen tube length during a specific growth period. Both sugar metabolism and ATP concentration were affected by sucrose shortage when pollen tubes were grown in glycerol-based media; this was related to decreases in the concentrations of glucose, fructose and UDP-glucose. The intracellular pH and ROS levels also showed a different distribution in pollen tubes grown in sucrose-depleted media. Changes were also observed at the cell wall level, particularly in the content and distribution of two enzymes related to cell wall synthesis (sucrose synthase and callose synthase). Furthermore, both callose and newly secreted cell wall material (mainly pectins) showed an altered distribution corresponding to the lack of oscillatory growth in pollen tubes. Growth in glycerol-based media also temporarily affected the movement of generative cells and, in parallel, the deposition of callose plugs.
• **Conclusion** Pollen tubes represent an ideal model system for studying metabolic pathways during the growth of plant cells. In our study, we found evidence that glycerol, a less energetic source for cell growth than sucrose, causes critical changes in cell wall deposition. The evidence that different aspects of pollen tube growth are affected is an indication that pollen tubes adapt to metabolic stress.

Key words: *Nicotiana tabacum*, pollen tube, sucrose, glycerol, callose, cellulose, sucrose synthase, cell wall, tip growth.

INTRODUCTION

Pollen grains, the male gametophyte of flowering plants, are unusual cells because they contain additional cells (the generative or sperm cells), which are in turn delimited by their own cell wall and plasma membrane. Pollen grains and pollen tubes are responsible for delivering sperm cells to the embryo sac, an essential process for sexual reproduction (Malho *et al.*, 2006). Pollen tubes grow exclusively at the apex using a specialized form of polar growth, known as 'tip growth'. Active intracellular streaming carries the cytoplasmic content (including gametes) towards the tube tip. To support this extremely rapid growth, pollen tubes require energy (Selinski and Scheibe, 2014). Carbohydrates and other storage compounds initially present in mature pollen are sufficient to support pollen survival and germination (Rodriguez-Garcia *et al.*, 2003; Nashilevitz *et al.*, 2009; Obermeyer *et al.*, 2013; Zienkiewicz *et al.*, 2013), but pollen tubes also require the uptake of external carbohydrate to support growth (Reinders, 2016). Since pollen tubes are fast-growing, photosynthetically inactive cells, an active respiratory and/or fermentative metabolism is required to support fast growth.

The metabolism of pollen tubes (such as those of lily) is characterized by at least three different phases of respiration. A first, rapid phase occurs before germination and takes ~30 min; the second phase is characterized by decreasing respiration rate during germination, while the third phase is characterized by a further increase in the respiration rate (Rounds *et al.*, 2011*b*). During the pre-germination step, cells showed a high rate of conversion of sugar to starch, suggesting that cells are preparing for the high energy demand of the next phases. Respiration is not likely to be sufficient because pollen tube growth is also supported by fermentation (Obermeyer *et al.*, 2013). In fact, when respiration is inhibited, growth is briefly stopped but restarted using aerobic fermentation as energy source (Rounds *et al.*, 2010). In the pollen of tobacco (*Nicotiana tabacum*), high respiration rates correspond to a significant level of ethanolic fermentation (Mellema *et al.*, 2002).

The energy demand of pollen tubes is initially maintained by internal storage (mainly starch), but subsequently it is supported by intake of external carbohydrates, mainly sucrose. Sucrose may enter pollen tubes through two routes. It can be catabolized

into fructose and glucose through invertase (Goetz *et al.*, 2016) or it enters using specific transporters (Lemoine *et al.*, 1999; Stadler *et al.*, 1999; Hirose *et al.*, 2010). Monosaccharides can be directed towards glycolysis and then respiration and/or fermentation, while sucrose can also be converted into UDP-glucose through the enzymatic action of sucrose synthase (Persia *et al.*, 2008). In the pollen tube, sucrose synthase is present in both the cytoplasm and the plasma membrane (in addition to the cell wall). Distribution of the enzyme is likely dependent on its phosphorylation status as well as on sucrose level, which affects the binding of sucrose synthase to actin filaments (Persia *et al.*, 2008). Production of UDP-glucose (which can also be obtained from glucose) is important because this metabolite is the precursor of callose and cellulose.

Callose, the most abundant cell wall component of pollen tubes, is produced by callose synthase, which is initially accumulated in Golgi-derived membranes and then delivered to the plasma membrane (Cai *et al.*, 2011). The enzyme is inserted in the plasma membrane in an inactive state, but it is activated by proteolytic events (Brownfield *et al.*, 2008). The role of callose is most likely to strengthen the cell wall of pollen tubes by forming a non-deformable sheath that counterbalances the turgor pressure (Williams, 2008; Winship *et al.*, 2011). Turgor pressure is most probably a consequence of membrane potential maintained by the activity of transmembrane proton ATPases (Pertl *et al.*, 2010; Lang *et al.*, 2014). The latter are most likely also responsible for regulating the pH gradient at the apex and are likely involved in the deposition of callose plugs (Certal *et al.*, 2008).

Energy production (in the form of ATP) is also required for the synthesis of other cell wall components, such as cellulose and pectins. Pectins are synthesized in the Golgi bodies and then secreted via secretory vesicles that fuse specifically at the pollen tube apex (Wang *et al.*, 2013), thereby allowing extension at the tip (Gu and Nielsen, 2013). Transport of Golgi and secretory vesicles, driven by the cooperation between actin filaments and microtubules (and associated proteins), is an additional energy-demanding process (Cai *et al.*, 2015).

The flow of energy, from uptake of sugars to their catabolism and then cell wall synthesis, requires a regulatory mechanism that must be necessarily interfaced with external signals and with the predetermined developmental programme of pollen tubes to precisely adjust the growth process both spatially and temporally. A primary role is played by the precise balance of ions and pH that accumulate preferentially in specific areas, thereby contributing to the polarization of pollen tubes (Winship *et al.*, 2017). Moreover, a different distribution of ROS and pH values between the tube apex and subapex are considered essential for the correct growth of pollen tubes. Generally, protons are distributed unevenly, forming an intracellular gradient with slightly acidic pH values at the extreme apex and probably an alkaline band in the subapical domain (Feijò *et al.*, 1999). The specific role of the proton gradient is still unclear, but it might be correlated with the activity of actin-depolymerizing factors (Chen *et al.*, 2002). The pH gradient in pollen tubes is presumably the result of the influx of protons at the apex and their efflux at the subapex due to plasma membrane-associated H^+-ATPase, the activity of which is also connected with the periodic deposition of callose plugs (Certal *et al.*, 2008). Changes in extracellular proton concentration might also regulate the activity of pectin-methyl esterase (PME), the enzyme that converts methyl-esterified pectins into acid pectins (Li *et al.*, 2002). Reactive oxygen species (ROS) are an inevitable consequence of aerobic metabolism, but are also generated in a controlled manner and used for a variety of functions, including pathogen defence and cell signalling. They are probably involved in the germination and growth of pollen tubes (Speranza *et al.*, 2012; Smirnova *et al.*, 2014). Reactive oxygen species are produced by enzymes such as NADPH oxidase at the apex of the pollen tube, and their production rate is strongly affected by Ca^{2+} (Potocky *et al.*, 2007, 2012) and other factors, such as polyamines (Aloisi *et al.*, 2015).

The *in vitro* growth of pollen tubes is therefore an ideal model system for studying the metabolic pathways of plant cells. Because pollen tubes do not have chloroplasts (hence the metabolic contribution of respiration cannot be confused with photosynthesis), they are heterotrophic cells and import large quantities of sugars from extracellular environments. The simplicity of this cell model makes it possible to study the effects of carbon depletion by monitoring the effects on the germination and growth of pollen tubes and on levels of metabolites such as ATP and sugars. In this work, we have studied how the replacement of sucrose with less metabolizable energy compounds (glycerol) can affect the development of pollen tubes. The aim was to investigate how pollen tubes adapt from a metabolic and cellular point of view to the lack of energy. We analysed the distribution of pH and ROS as well as cell wall assembly by monitoring specific polysaccharides and the cytological distribution of two critical enzymes (sucrose synthase and callose synthase). In addition, we tested how metabolic stress affects the primary function of pollen tubes, i.e. the transport of gametes.

MATERIALS AND METHODS

Pollen growth in different media

Seeds of *Nicotiana tabacum* (tobacco) were from the Seed and Plant Collection of the Botanical Garden at Siena University. Tobacco plants were grown under standard conditions in greenhouses and pollen was collected from opening flowers from June to August; pollen was dehydrated and stored at −20 °C. When needed, pollen was hydrated at room temperature over night in a moist chamber, then the pollen was placed in four different growth media: (1) BKS, BK medium supplemented with 12 % sucrose (Brewbaker and Kwack, 1963); (2) BKP, BK medium with 13 % polyethylene glycol 3350 (PEG); (3) BKM, BK medium with 11 % maltose; (4) BKG, BK medium with 3.3 % glycerol.

We measured the germination rate and length of at least 100 pollen tubes in all assays to statistically evaluate both parameters. Growth media were chosen to maintain the osmolarity when compared with control (i.e. BK with 12 % sucrose). We referred to data presented in Zerzour *et al.* (2009). First, the growth rate was tested for each selected medium within 150 min; images of growing pollen tubes were taken at different intervals. For each image, we measured the length of germinated tubes using ImageJ software (https://imagej.nih.gov/ij/index.html) to evaluate the growth rate. Subsequently, we

measured the growth rate of pollen tubes grown in BKS and BKG (the growth media selected) for 7 h, measuring the pollen tube length at intervals of 60 min.

Protein extraction from cytosol, membranes and cell wall

We extracted proteins of pollen tubes from three different intracellular compartments: the cytosol, the membranes and the cell wall. The extraction protocol was performed for pollen grown in BKS and BKG at three different germination times: 4, 5 and 6 h (the logic behind the choice of these three intervals is explained later). After germination, 500 mg of pollen was collected and centrifuged at 135 *g* for 5 min, then washed with HEMS or HEMG buffer (50 mM HEPES pH 7.5, 2 mM EGTA, 2 mM $MgCl_2$, with either 12 % sucrose [HEMS] or 3.3 % glycerol [HEMG])

After washing, samples were centrifuged again at 135 g for 5 min, the supernatants were discarded and lysis buffer (50 mM HEPES pH 7.5, 2 mM EGTA, 2 mM $MgCl_2$, protease inhibitors, 1 mM dithiothreitol) was added to the pellets. Mechanical lysis of pollen was carried out in a cold room (4 °C) using a Potter-Elvehjem homogenizer with 40 strokes. Samples were then centrifuged at 500 *g* for 10 min at 4 °C; pellets and supernatants were subjected to different processes. Pellets, containing cell wall proteins, were washed three times with HEM buffer by centrifuging at 15 000 *g* for 10 min at 4 °C after each wash. The last pellet (referred to as the 'cell wall sample') was resuspended with Laemmli sample buffer (Laemmli, 1970) for 1-D electrophoresis. The supernatants, containing both cytosol and membrane proteins, were centrifuged at 100 000 *g*, 4 °C, for 45 min. The resulting pellets (referred to as the 'membrane sample') were resuspended with Laemmli sample buffer; the corresponding supernatants were supplemented with 4 volumes of 20 % TCA in cold acetone (with 0.07 % 2-mercaptoethanol) to allow protein precipitation overnight at −20 °C. After precipitation, samples were centrifuged at 15 000 *g* for 15 min at 4 °C, the supernatants were discarded and the pellets were washed twice with 100 % cold acetone (with 0.07 % 2-mercaptoethanol) and resuspended in Laemmli sample buffer. The final sample is referred to as the 'cytosol sample'.

Determination of protein concentration

The protein concentration of samples was determined using a commercial kit (2-D Quant Kit, GE HealthCare). The protocol was performed exactly as described in the instruction manual using BSA as reference. Each sample was analysed in three replicates using a Shimadzu UV-160 spectrophotometer at 480 nm.

1-D electrophoresis

Separation of proteins by 1-D electrophoresis was performed on precast gel (Criterion Tris–HCl PreCast Gel, 10 %, Bio-Rad) using a Criterion cell (Bio-Rad) equipped with a Bio-Rad PowerPac 300 at 200 V for ~55 min. Gels were run according to Laemmli (1970) using TGS (25 mM Tris–HCl pH 8.3, 192 mM glycine, 0.1 % SDS) as running buffer. Gels were stained with Bio-Safe Coomassie blue (Bio-Rad) as described in the instruction protocol.

Western blotting and image analysis

Transfer of proteins from gels to nitrocellulose membranes was performed using a Trans-Blot Turbo Transfer System (Bio-Rad) according to the manufacturer's instructions. Quality of blotting was determined by checking the transfer of precision pre-stained molecular standards (Bio-Rad). After blotting, membranes were blocked overnight at 4 °C in 5 % ECL Blocking Agent (GE HealthCare) in TBS (20 mM Tris pH 7.5, 150 mM NaCl) plus 0.1 % Tween-20. After washing with TBS, membranes were incubated with the primary antibodies for 1 h at room temperature. The antibody to sucrose synthase was used at the dilution of 1:1000 (Persia *et al.*, 2008) while the antibody to callose synthase was diluted 1:300 (Cai *et al.*, 2011). Subsequently, membranes were washed several times with TBS and then incubated for 1 h with anti-rabbit immunoglobulin G peroxidase-conjugated secondary antibodies, purchased from Bio-Rad and diluted 1:5000. Blots were finally incubated with the Clarity reagents (Bio-Rad). Images of gels and blots were acquired using a Fluor-S apparatus (Bio-Rad) and analysed with Quantity One software (Bio-Rad). Exposure times were 30–60 s for blots and 5–7 s for Coomassie-stained gels.

Analysis of blots was performed with Quantity One software. All blots were developed using identical conditions from substrate incubation to exposure time. All images were processed correspondingly using the Autoscale command (to improve the quality of gels and blots) and the Background Subtraction command (to remove the background noise). The relative intensity of single spots was calculated with the Volume tool of Quantity One software. Blots were performed in triplicate. Results were exported and graphed with Microsoft Excel.

Kymograph analysis of pollen tubes

Growing pollen tubes were observed using an inverted microscope (Diaphot TMD) with a 40× objective (Nikon). Video sequences of growing pollen tubes were captured using a CCD camera (C2400-75i, Hamamatsu Photonics) connected to an Argus-20 processor (Hamamatsu) and then to a video capture system (Cai *et al.*, 2000). Video clips of pollen tubes were captured as MPEG-2 files at a resolution of 720 × 576 pixels using the software PCTV Center. MPEG-2 files were converted to AVI (MJPEG compression) with the software VirtualDub (http://virtualdub.org/) and then opened in ImageJ software (http://rsbweb.nih.gov/ij/index.html).Video sequences were analysed with the plugin Kymograph (written by Jens Rietdorf, FMI, Basel, and Arne Seitz, EMBL, Heidelberg) to measure the speed of moving objects in a series of images. During kymograph analysis, we analysed and measured the grey values in each region of interest (ROI) selected manually for each frame in the image series. A new image (a kymograph or space–time graph) was generated, in which the *x*-axis is the time axis (the unit is represented by the frame interval) while the *y*-axis indicates the movement rate of the ROI (the unit of measurement

is the distance in pixels travelled by the object). The speed of objects was measured directly by the plugin. At least 20 pollen tubes for each sample were analysed.

Immunofluorescence microscopy

Indirect immunofluorescence microscopy in pollen tubes was performed according to standard procedures (Cai *et al.*, 2011). After fixation with 3 % paraformaldehyde in PM buffer (50 mM PIPES pH 6.9, 1 mM EGTA, 0.5 mM $MgCl_2$) for 30 min, 50 mg of pollen sample was washed with PM for 10 min and then incubated with 1.5 % Cellulysin (Sigma) for 7 min in the dark. After two washes with PM buffer, samples were incubated with the primary antibodies. The anti-sucrose synthase antibody (Heinlein and Starlinger, 1989; Persia *et al.*, 2008) was used at 1:100 dilution while the anti-callose synthase antibody was used at 1:50. Antibodies were incubated at 4 °C overnight. Following two washes with PM buffer, samples were incubated with a goat anti-rabbit secondary antibody conjugated to Alexa Fluor 488 (Invitrogen) diluted 1:150 for 45 min in the dark. Antibodies JIM5 (against acid pectins) and JIM7 (against methyl-esterified pectins) were purchased from PlantProbes (http://www.plantprobes.net). Both antibodies were used at 1:5 dilution for 3 h at room temperature. For JIM5 and JIM7 antibodies, incubation with Cellulysin was not carried out. As secondary antibody, a goat anti-rat antibody conjugated with Alexa 594 was used, diluted 1:50 and incubated for 45 min at 37 °C. After two washes in PM buffer, samples were placed on slides and covered with a drop of Citifluor. Observations were made using a Zeiss Axio Imager microscope with a 63× objective. Images were acquired with an AxioCam MRm camera using the software AxioVision. Images of higher quality were obtained using structured illumination. In controls, primary antibodies were omitted. For the measurement of fluorescence intensity in the cell border, original ZVI files generated by the AxioVision software were imported into ImageJ and the signal intensity was measured with a segmented line sufficiently wide to cover the signal (~2 µm) by starting from the apex of pollen tubes in the direction of the pollen grain. The obtained measure was normalized against the background by selecting a large area outside the pollen tube. To quantify the intracytoplasmic fluorescence signal, individual images were imported into ImageJ and a segmented line was depicted to cover the ROI. The line thickness was such that it largely occupied the cell cytoplasm. The signal was measured with the Analyze > Plot profile command.

Analysis of newly secreted cell wall material, generative cell movement, pH and ROS

Labelling of newly secreted cell wall material was performed using propidium iodide (PI). Rounds *et al.* (2011*a*) showed that levels of PI fluorescence matched those of GFP-labelled pectin methyl esterase. The authors also showed competitive reduction of PI fluorescence after binding of Ca^{2+} to pectins (indicating that PI fluorescence reflects pectin binding). Despite some evidence that PI may label pectins, it is more significant that PI labels the area where new cell wall material is secreted. Measurement of PI fluorescence was performed along the cell edge using the Segmented Line tool of ImageJ with a selection width of ~2 µm. After subtracting the background (as measured in representative pollen tubes), we calculated the average values and standard deviation.

The generative cell test was performed using 4′,6-diamidino-2-phenylindole (DAPI) staining in pollen tubes grown in both sucrose- and glycerol-based media. We analysed the generative cell movement for 4 consecutive hours, after 3 h of germination. Pollen tubes were placed on glass slides and then stained with DAPI; after a few minutes of incubation, observations were made using a Zeiss Axio Imager fluorescence microscope equipped with a 63× objective. Images were captured with an MRm AxioCam video camera using AxioVision software. ZVI files were opened in ImageJ, which was used to measure the total length of pollen tubes and the distance covered by generative cells from the pollen grain. To statistically evaluate our observations, we performed two consecutive tests: first, we analysed the data by analysis of variance (ANOVA); secondly, we performed Student's *t*-test. In both cases, we used the Data Analysis module of Excel software.

The BCECF-AM [2′,7′-bis-(2-carboxyethyl)-5-(and-6)-carboxyfluorescein, acetoxymethyl] ester probe was used to visualize the proton levels (i.e. pH) in tobacco pollen tubes (Fricker *et al.*, 1997). A final concentration of 5 µM was obtained from a dimethyl sulphoxide (DMSO) stock solution of 1 mM; the required volume was directly added to both the sucrose and the glycerol germination medium. The cytosolic pH was immediately visualized (within 5 min) after addition of the probe to prevent uptake of the pH probe by organelles.

We detection ROS as described by Aloisi *et al.* (2015) using the fluorescent ROS indicator dye 2′,7′-dichlorodihydrofluorescein diacetate (DCFH2-DA; Molecular Probes). Samples were observed with a Zeiss Axio Imager fluorescence microscope equipped with a 63× objective, an MRm AxioCam video camera and structured illumination. Control of the ROS probe involved the absence of the probe itself (no signal except for the autofluorescence of pollen grains) and the addition of fluorescein diacetate (in which case we observed a signal uniformly diffused throughout the pollen tube) (not shown).

To highlight the differences in fluorescence intensity between different regions of pollen tubes, when necessary single grey-scale images were transformed into pseudocoloured images using ImageJ software, specifically the command Image > Lookup tables > 16 colours.

Immunogold electron microscopy

Immunogold labelling of tobacco pollen tubes was performed according to the protocol described in Li *et al.* (1995). The antibody to callose synthase was used at the dilution of 1:100 in 50 mM Tris–HCl pH 7.6, 0.9 % NaCl, 0.1 % Tween 20, 0.2 % BSA. The goat anti-rabbit secondary antibody was conjugated with 15 nm gold particles (BioCell). Images were captured with a Philips Morgagni 268 D transmission electron microscope (TEM) set at 80 kV and equipped with a MegaView II CCD camera (Philips Electronics, Eindhoven, The Netherlands). Samples were incubated with 5 % normal goat serum (Invitrogen) for

20 min at room temperature to prevent binding to non-specific sites. Sections were incubated with the primary antibody for 1 h and then washed (three or four times) in 50 mM Tris–HCl pH 7.6, 0.9 % NaCl, 0.1 % Tween 20 for 30 min. After drying, samples were incubated with the gold-conjugated secondary antibody for 15 min at room temperature. After washing for 30 min and in H_2O for 10 min, sections were counterstained with 2 % uranyl acetate in H_2O for 10–20 min, carefully washed in H_2O for 15 min and then counterstained with lead citrate for 5–10 min.

Analysis of ATP/ADP and sugars by high-performance liquid chromatography (HPLC)

We analysed ATP and ADP by HPLC (Perkin Elmer Series 200) following the method tested by Liu *et al.* (2006). Fifty milligrams of pollen was collected by centrifugation at 135 *g* for 5 min from both sucrose and glycerol germination media at regular intervals of 1 h and resuspended in boiling water (1 mL). Complete disintegration and rupture of cells were performed with a Potter-Elvehjem homogenizer with 40 strokes per sample. The homogenate was centrifuged at 15 000 *g* for 15 min at room temperature. The supernatants were transferred to vials and 20 µL of sample was injected into a solid stationary-phase C18 column (75 × 4.6 mm, particle size 5 µm). The mobile phase was a binary mobile phase gradient (solvent A, 10 mM phosphate buffer pH 7; solvent B, acetonitrile) with the following gradient: 0 min, 100 % solvent A, 0 % solvent B; 2 min, 95 % A, 5 % B; 4 min, 80 % A, 20 % B; 5.3 min, 75 % A, 25 % B; 6 min, 100 % A, 0 % B. The following parameters were used: flow rate 0.3 mL min^{-1}; room temperature; approximate elution time 6 min for ATP and 7 min for ADP. Identification of different components was obtained by programming a DAD 235C spectrophotometric detector with excitation wavelength 254 nm.

Sugar analysis was performed by lysing pollen as described above; the final supernatants were examined by isocratic HPLC analysis with a Waters Sugar-Pak I ion-exchange column (6.5 × 300 mm) at a temperature of 90 °C and using a Waters 2410 refractive index detector. MilliQ grade water (pH 7) was used as a mobile phase with a flow rate of 0.5 ml min^{-1}; an injection loop of 20 µL was used for all samples and standards (sucrose, glucose and fructose).

RESULTS

Germination rate and length of pollen tubes are affected by growth medium

To understand whether replacement of sucrose with another carbon source can affect pollen metabolism and growth, we initially measured the germination rate and length of pollen tubes (Fig. 1) while growing in four different germination media. First, we measured the pollen tube length after growing for 150 min (Fig. 1A). We found that pollen grains germinated normally in the presence of sucrose (as standard condition), while use of maltose and PEG did not show relevant differences in pollen tube length. On the contrary, we found a significant reduction in the length of pollen tubes grown in glycerol-supplemented media (Fig. 1A). Reduction in length was clear after 120 min of growth and statistical analysis showed that length was significantly different from 100 min of growth onwards (asterisks). Because we were looking

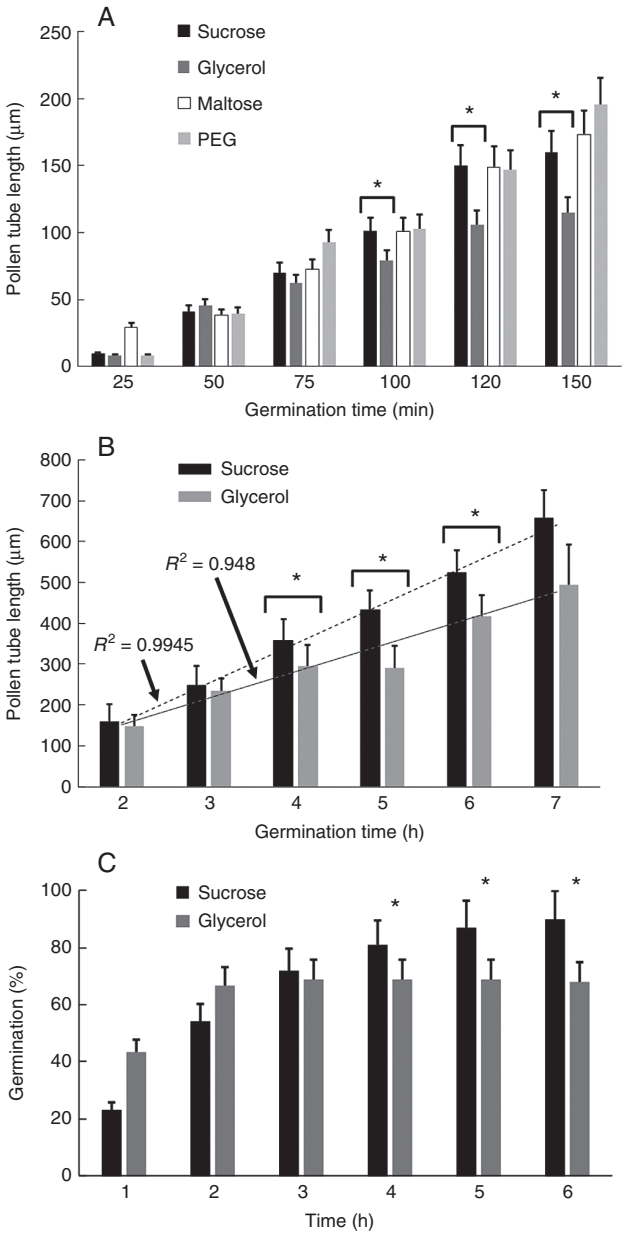

FIG. 1. Pollen tube growth under standard conditions and in the presence of different osmotic compounds. (A) Pollen tube growth in BK medium supplemented with different osmotic molecules (sucrose, glycerol, maltose, PEG). The analysis was carried out for 150 min. Statistically significant differences were observed between growth in sucrose- and glycerol-based media (in all the panels the asterisks correspond to P <0.05). Bars indicate standard deviation. (B) Analysis of pollen tube length after growth in BK medium supplemented with either sucrose or glycerol. The analysis was carried out for 7 h. Statistically significant differences were determined after 4, 5 and 6 h of germination (asterisks). For both analyses, trend lines and corresponding R^2 values are reported. (C) Analysis of germination of pollen tubes in BK medium supplemented with either sucrose or glycerol. This parameter was monitored for 6 h. Asterisks indicate the time points when germination in BK medium plus sucrose was statistically higher than that in BK medium plus glycerol.

for pollen tubes metabolically inhibited by scarcity of carbon source, we continued the analysis only using sucrose- and glycerol-based media.

We proceeded by testing the growth of pollen tubes for longer times (up to 7 h). While pollen tubes grown in sucrose-based medium exhibited a typical tube elongation rate (up to 350 µm after 7 h), the length of pollen tubes grown in glycerol-based medium was significantly reduced. Statistical analysis showed that the length of pollen tubes grown in glycerol-based medium was different after 4 h of growth until 6 h of growth. After 7 h of growth, pollen tubes in glycerol-based medium increased their growth rate. The difference between sucrose- and glycerol-based media was also confirmed by analysis of linear regression as reported in Fig. 1B. In sucrose-based medium, pollen tube length increased linearly ($R^2 = 0.9945$) while in glycerol-based medium the value of R^2 was typically around 0.948.

The germination rate of pollen grains also changed significantly; while in sucrose-based medium we observed a higher percentage of germinated pollen (around 85–90 %) after 6 h, in glycerol-based medium we found that pollen grains germinated faster than the control after 1 h of incubation, but germination rate slowed down significantly after 4 h because the percentage of germinated grains remained stable but lower than in the control (Fig. 1C).

The growth rate of pollen tubes was also subjected to kymographic analysis. In the standard condition (Fig. 2A) the speed of growth was constant, as shown by the linearity of the kymograph profile. In the example illustrated, the pollen tube showed a growth speed of ~1.37 µm min^{-1}. In addition, it was possible to observe the typical oscillation of growth, i.e. slower phases of growth preceded/followed by peaks of fast growth (the oscillation between slow and rapid growth phases is shown by the magnification of a kymograph of a control pollen tube in Fig. 2C). When pollen grains were grown in glycerol-based medium (Fig. 2B) the speed of growth was different, as shown by the kymograph profile. We observed different speeds of growth because pollen tubes were growing like the controls during the first 2–3 h (1.3–1.5 µm min^{-1}) but their growth rate decreased significantly compared with controls soon after (to 0.6 µm min^{-1}). After 6 h of growth, the growth rate increased again, to 1.3 µm min^{-1}. In addition, we did not detect any oscillation in the growth rate, as depicted in the magnification of the kymograph of a metabolically stressed pollen tube in Fig. 2D. The difference in growth rate is more appreciable in Fig. 2E. In glycerol-based medium, the growth rate of pollen tubes decreased significantly after 180–200 min but increased again after 6 h of growth. Interestingly, around 500 min (~8 h of growth) the elongation rate was comparable to controls in sucrose-based medium.

ATP/ADP and sugar concentrations changed in different growth conditions

In order to get a first assessment of the metabolic state of pollen tubes grown in the two different media, we analysed the concentrations of ATP/ADP and the main sugars (glucose, fructose and UDP-glucose) in pollen tubes. All metabolites were analysed using HPLC during the first 6 h of growth. We found clear differences in ATP concentrations between pollen tubes grown in sucrose- and glycerol-based media. The ATP concentration was relatively constant for the first 4 h in sucrose-based medium and slightly decreased after the fifth and sixth hours of growth. On the contrary, in glycerol-based medium the ATP concentration decreased specifically during the first 2 h of growth and progressively stabilized at lower levels at the end of treatment. The concentration of ADP was found to be relatively constant in both treatments; in fact we did not find any significant change, and generally the amount of ADP was lower in glycerol-based medium than in sucrose-based medium (Fig. 3A).

We also investigated the concentrations of three important sugars of pollen tubes, namely UDP-glucose, glucose and fructose. The concentration of UDP-glucose during pollen tube growth in both media remained relatively constant for 6 h; nevertheless, the relative concentration of UDP-glucose in pollen tubes grown in sucrose-based medium was consistently and significantly higher than that observed in pollen tubes grown in glycerol-based medium (Fig. 3B). However, no specific trend of variation could be deduced from the measurements. Further analysis concerned the relative quantity of glucose and fructose in pollen tubes grown in two different media. In standard conditions, the relative concentrations of both monosaccharides increased during growth (Fig. 3C) probably because of progressive cleavage of sucrose. On the contrary, in glycerol-based medium the concentrations of both sugars oscillated similarly during growth, with a peak of concentration after 3–4 h of growth. At the first hour of analysis, the relative concentration of these monosaccharides was below the limit of instrumental detection. In any case, the most striking difference concerned the relative concentrations between sucrose- and glycerol-based media because in the latter concentration the values were at least a few hundred times lower than those measured in sucrose-based medium (Fig. 3D).

Distribution of pH and ROS is affected by growth medium

Variations in pH can affect the expansion of apical-growing cells. Therefore, to understand whether different media might affect pH values in pollen tubes, we analysed the pH distribution in pollen tubes grown for 5 h (the time during which major effects on growth were observed) in both sucrose- and glycerol-based medium. We found that pH in pollen tubes grown under standard conditions was low (acid) at the apex and increased (thus more basic) in the subapex and shank of pollen tubes (Fig. 4A; left panel, bright field; right panel, fluorescence). On the contrary, pollen tubes grown in glycerol-based medium showed a relevant difference because pH was relatively constant along the tube and no clear differences could be appreciated (Fig. 4B; left panel, bright field; right panel, fluorescence). To confirm such observations, we also measured the fluorescence signals from the very tip down along the tube axis. The corresponding graph, as obtained by analysing the fluorescence signal of several pollen tubes and by normalization against the background, illustrates the differences in pH distribution between the two growth media (Fig. 4C). In both graphs, the measured values were compared with the highest observed value (set as 100 %).

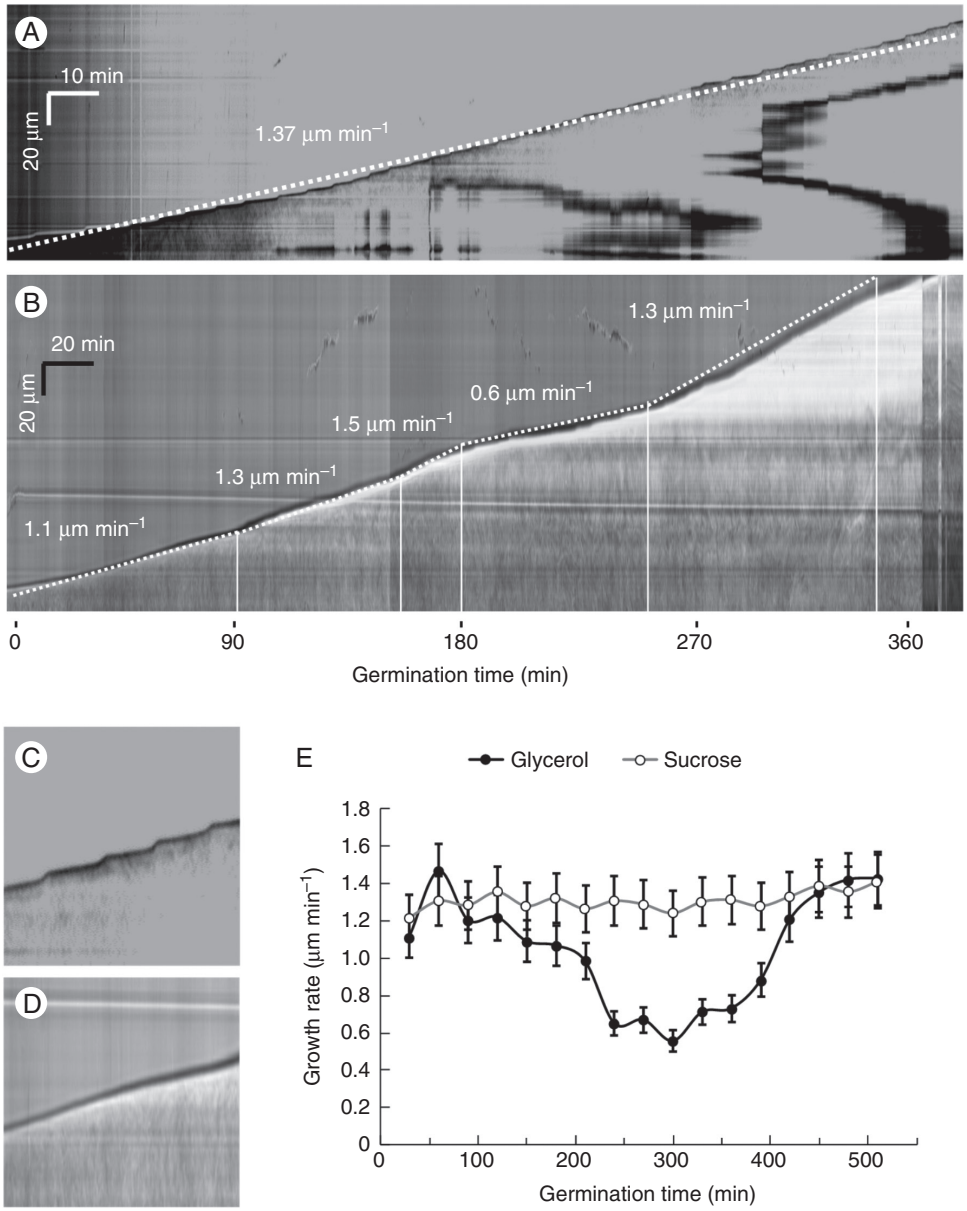

FIG. 2. Growth of pollen tubes as analysed by kymography in BK medium supplemented with either sucrose or glycerol. (A) Typical growth profile of pollen tubes in BK medium plus sucrose. The velocity reported in the image refers to a frequently observed average value. Time and distance bars are shown at the top left. (B) Kymographic analysis of pollen tubes grown in BK medium plus glycerol. The growth pattern was arbitrarily divided into segments in which speed was relatively constant. The values shown indicate average speeds for each segment. Note the marked decrease in growth after the third hour of germination. Time and distance bars are shown at the top left. (C, D) Detail of the growth profile of pollen tubes in BK medium plus sucrose (C) or plus glycerol (D). Note the oscillatory profile in C as opposed to the linear profile in D. (E) Analysis of average growth speed as calculated by kymography. Note the minimum growth value around the fifth hour in BK medium plus glycerol.

Results obtained after analysis of ROS distribution were substantially like those obtained for the pH analysis. Pollen tubes grown for 5 h in sucrose-based medium were characterized by a high concentration of ROS in the apical region (the first 10–15 µm) while the subapical and shank regions were poor in ROS (Fig. 5A; left panel, bright field; right panel, fluorescence). Conversely, the distribution of ROS in pollen tubes grown for 5 h in glycerol-based medium was substantially different because it was quite uniform throughout the pollen tube (Fig. 5B; left panel, bright field; right panel, fluorescence). A statistical analysis of the data confirmed the visual interpretation; pollen tubes grown in sucrose-based medium exhibited a remarkable peak of ROS at the apex (Fig. 5C, solid line) while pollen tubes grown in glycerol-based medium showed a very homogeneous distribution of ROS (Fig. 5C, dashed line).

Acidic and methyl-esterified pectins are differently localized in pollen tubes grown in different media

To deepen our understanding of the way in which pollen tubes grow, we monitored the secretion of new cell wall material at the

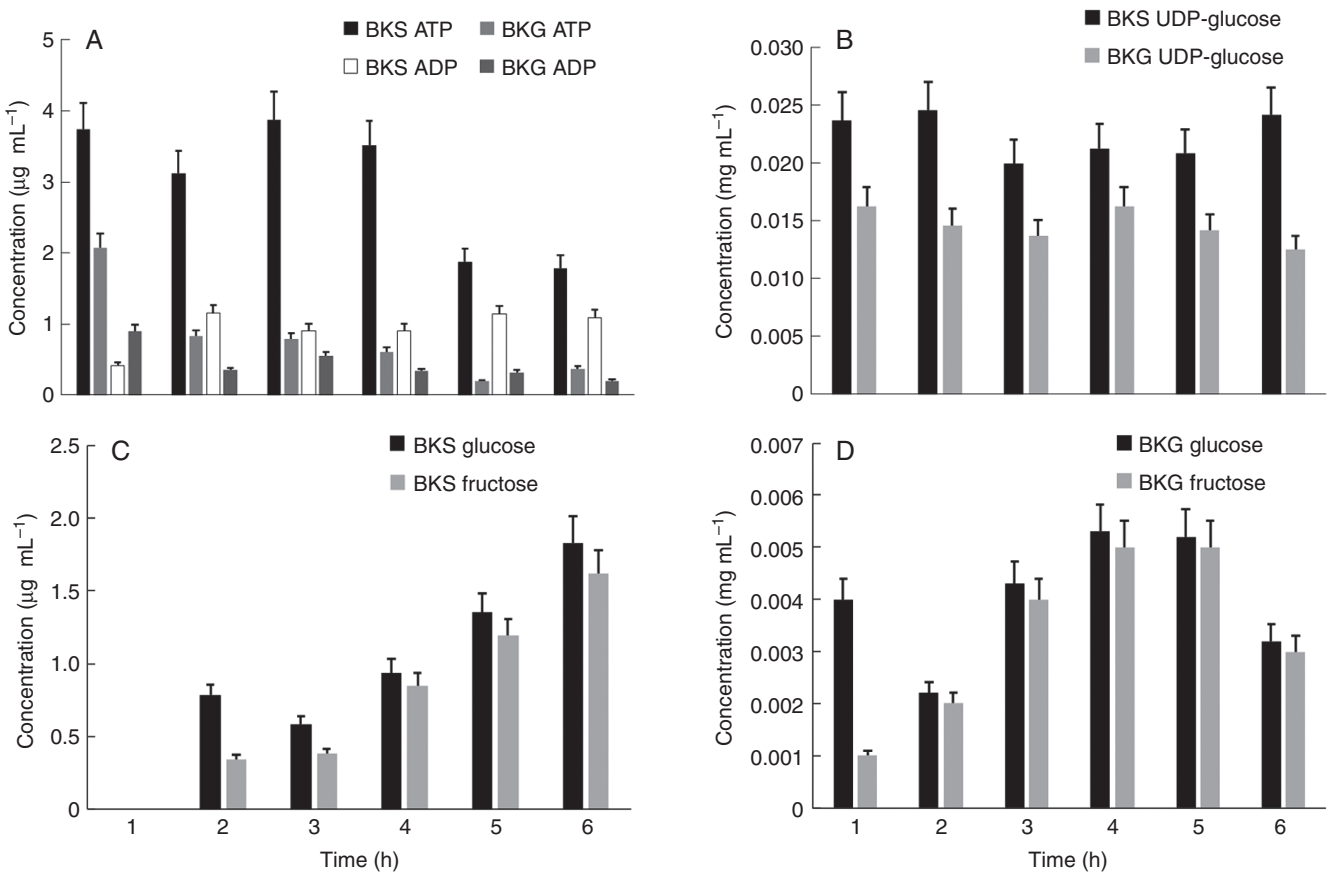

FIG. 3. Analysis of metabolites in pollen tubes grown in BK medium supplemented with sucrose or glycerol. The analysis was performed after each hour of germination for a period of 6 h. (A) Measurement of the concentrations of ATP and ADP in pollen tubes grown in BK plus sucrose (BKS) or plus glycerol (BKG). (B) Concentration analysis of UDP-glucose in the two experimental conditions. (C) Analysis of the concentration of glucose and fructose in pollen tubes grown in BK medium plus glycerol. No signal was found at the first hour because values were below the instrumental detection limit. (D) Analysis of glucose and fructose in pollen tubes grown in BK medium plus sucrose. In all cases, bars indicate the standard deviation.

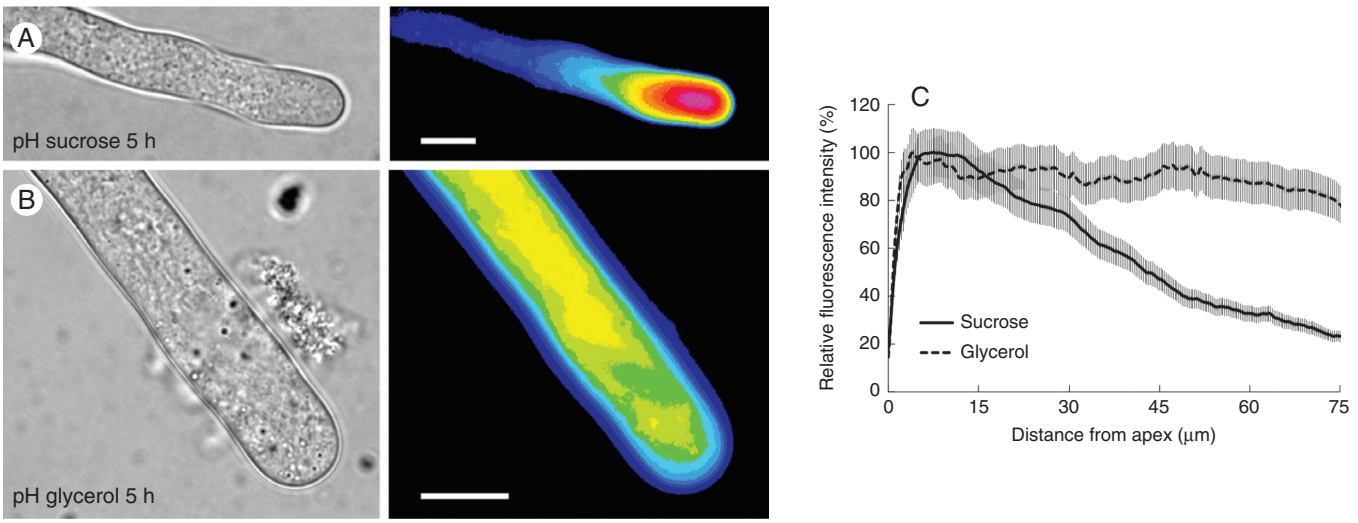

FIG. 4. Analysis of pH distribution in pollen tubes grown for 5 h in sucrose- and glycerol-based media. (A) The pH in pollen tubes grown under standard conditions is relatively low (acid) at the apex but increases (becomes more basic) in the subapex and shank of pollen tubes. (B) In pollen tubes grown in glycerol-based medium, the pH is relatively constant along the tube. (C) Measurement of the fluorescence signal from the apex along the axis of pollen tubes. The graph illustrates the differences in pH distribution in pollen tubes grown in different growth media. Values were normalized against the background and referred to the highest value, which was set as 100 %. Scale bars = 10 µm.

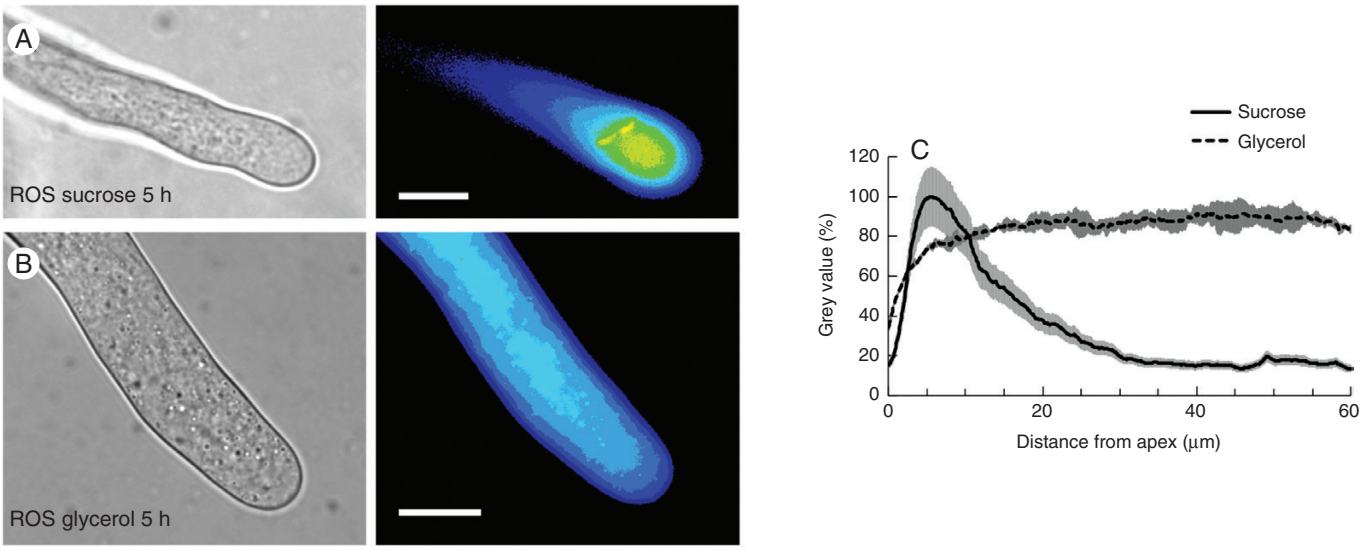

FIG. 5. Analysis of the presence of ROS in pollen tubes after 5 h of growth in BK medium plus sucrose or glycerol. (A) A pollen tube (left) and the corresponding fluorescence signal of the ROS probe (pseudocoloured, right) after 5 h of growth in BKS. (B) A pollen tube (left) and the corresponding fluorescent signal of ROS (pseudocoloured, right) after 5 h of growth in BKG. (C) Distribution profile of ROS as measured from the apex of pollen tubes grown in BKS (solid line) and BKG (dashed line). The grey areas along the two profiles indicate the standard deviation.

apex. Initially we used labelling with PI. After 5 h of growth, the cell wall material stained with PI accumulated mainly in the apical cell wall and, to a lesser extent, in the subapical cell wall of pollen tubes grown in sucrose-based medium (arrow in Fig. 6A). Unlike controls, pollen tubes grown for 5 h in glycerol-based medium showed a significant difference because the cell wall labelled with PI was homogeneous (Fig. 6B) and relatively similar between the apex/sub-subapex and the shanks of pollen tubes. This suggests the absence of preferential secretion/accumulation of newly synthesized pectins. To further investigate the pattern of pectin secretion, we labelled methyl-esterified pectins with JIM7 antibody and acidic pectins with JIM5 antibody. In sucrose controls, methyl-esterified pectins accumulated abundantly at the apex of pollen tubes and much less in distal regions (Fig. 6C). In contrast, the distribution of methyl-esterified pectins in glycerol-grown pollen tubes was relatively similar in different regions of pollen tubes (Fig. 6D). This difference in pectin distribution between sucrose- and glycerol-grown cells was confirmed by the analysis of acidic pectins. In pollen tubes grown in sucrose the antibody JIM5 provided a classic ring pattern (typical of pulsed growing pollen tubes) (Fig. 6E); this pattern of distribution was made clear by image analysis along the pollen tube axis, which highlighted the regularity of signal peaks of acidic pectins (Fig. 6F). In pollen tubes grown in glycerol, the ring pattern was maintained (Fig. 6G) but with two major differences, as shown by image analysis (Fig. 6H). Firstly, there was an intense signal at the apex of pollen tubes; secondly, signal peaks were much less intense, sometimes not discernible from background noise. This suggests that acidic pectins are more evenly distributed than sucrose controls.

Lack of sucrose changes the accumulation and localization of sucrose synthase in pollen tubes

As a next step in evaluating the adaptation of pollen tubes to new growing conditions, we analysed sucrose synthase as a critical enzyme in the allocation of carbon between respiration and cell wall synthesis. To get information on changes in protein content, we performed SDS–PAGE analysis of proteins extracted from pollen tubes grown for 4, 5 and 6 h in both sucrose- and glycerol-based media. Proteins were extracted from three different cell compartments, namely the cytosol (Fig. 7A), the cell wall (Fig. 7B) and the membranes (Fig. 7C). A preliminary visual analysis showed no significant difference in the protein pattern between different growth conditions or between different growth times within each cellular fraction. To investigate the accumulation rates of sucrose synthase, we analysed its relative content by immunoblot analysis of all fractions (Fig. 7D). The results confirmed that the relative content of sucrose synthase could be affected by metabolic stress. Specifically, we found that in the standard condition (sucrose-based medium) the accumulation of sucrose synthase was not homogeneous in the cytosol within the time of analysis, with a significant reduction after 6 h of growth (Fig. 7D, lanes 2–4). Comparatively, an uneven accumulation pattern could also be observed in the cell wall protein fraction (lanes 8–10), whereas membrane-associated sucrose synthase appeared to reach the highest amount after 5 h of growth in sucrose-based medium (lanes 14–16). These data indicate that the amount of sucrose synthase oscillated during the growth of pollen tubes. When the levels of sucrose synthase were analysed in the protein fractions of pollen tubes grown in glycerol-based medium, an uneven pattern of accumulation could be observed in the protein fractions from cytosol (lanes 5–7), cell wall (lanes 11–13) and membranes (lanes 17–19). To clarify whether oscillation in the levels of sucrose synthase was comparable between pollen tubes grown in either sucrose- or glycerol-based media, we compared different blot results quantitatively. In pollen tubes grown in sucrose medium, the amount of sucrose synthase in the cytosol and membranes decreased progressively from 4 to 6 h of growth, resulting in the accumulation of sucrose synthase in the cell

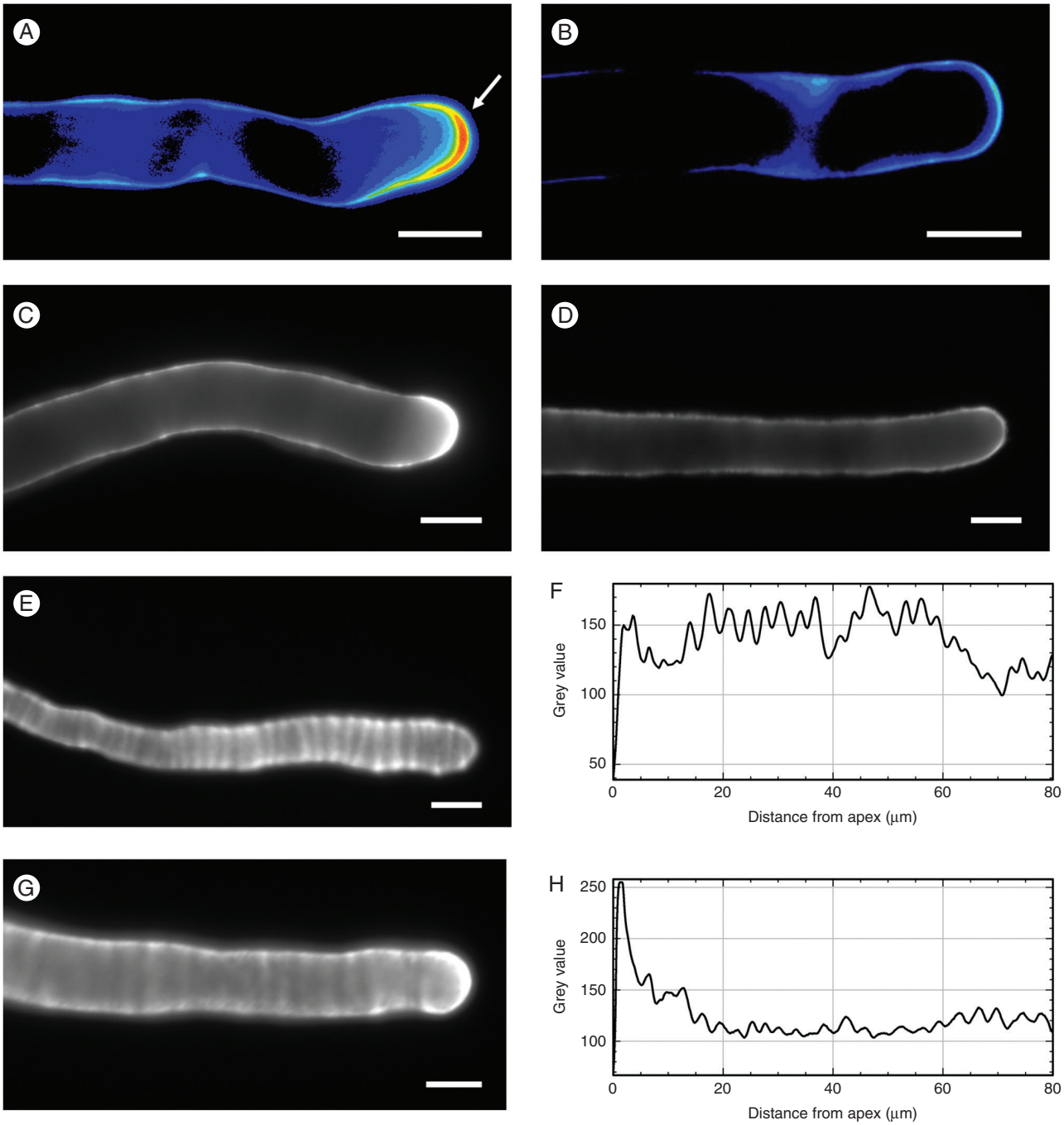

FIG. 6. Deposition of pectins in the cell wall. (A) Typical pollen tube grown in BKS medium and labelled with PI. Note the strong signal in the apical region of the pollen tube (arrow). (B) A pollen tube grown in BKG and labelled with the PI probe. The signal is homogeneous along the tube edge. (C) A typical pollen tube grown in BKS and labelled with JIM7 antibody; the apex is strongly stained. (D) A typical pollen tube grown in BKG and labelled with JIM7; the signal is homogeneous along the cell wall. (E) A pollen tube grown in BKS and labelled with JIM5 antibody; acidic pectins are distributed at regular intervals, as shown by the graph in (F). (G) A pollen tube grown in BKG and labelled with JIM5; as shown by the analysis in (H), acidic pectins accumulate at the apex and are more homogeneous along the pollen tube. Scale bars = 10 µm.

wall protein fraction (Fig. 7E). This kind of behaviour was not observed in pollen tubes grown in glycerol medium. In this case, the levels of sucrose synthase in the cytosol slightly decreased while the relative amount of cell wall-associated sucrose synthase remained constant and the levels of enzyme in the membrane fraction increased slightly.

Because sucrose synthase is present in different cellular sites of pollen tubes, we focused our attention on its distribution in the presence (control) and absence (medium with glycerol) of sucrose. Analyses were performed by immunofluorescence microscopy 5 h after germination (Fig. 8). Analysis of control samples (Fig. 8A) showed the typical distribution of the

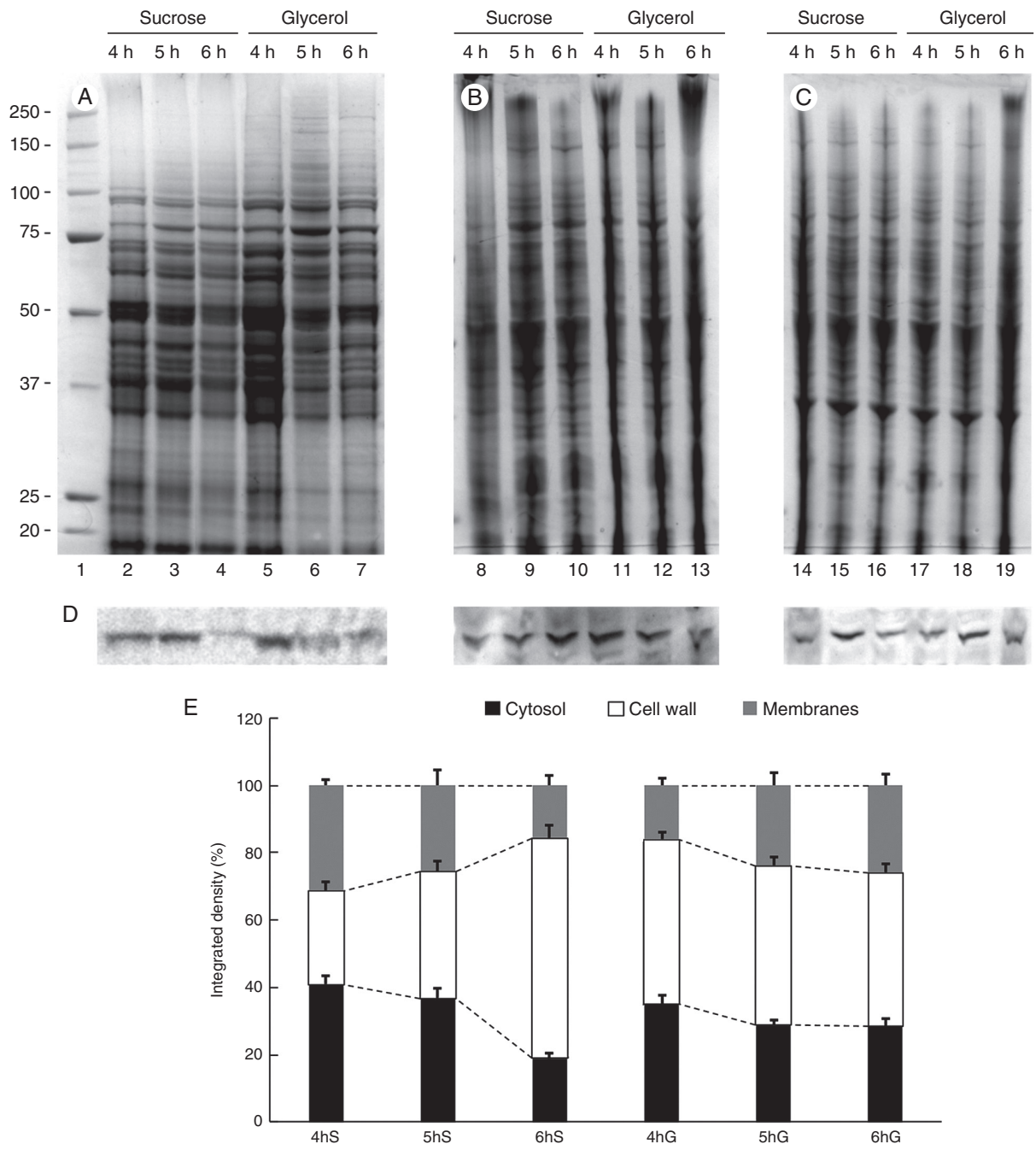

FIG. 7. Relative accumulation of sucrose synthase in the cytosol, membranes and cell walls of pollen tubes grown in BKS and BKG. (A) Electrophoretic analysis of proteins extracted from the cytosol of pollen tubes grown for 4, 5 and 6 h in the two different media. Molecular weight standards (kDa) are indicated on the left. (B) Profile of proteins extracted from the cell wall of pollen tubes grown for 4, 5 and 6 h in BKS and BKG. (C) Electrophoresis of proteins extracted from the membrane fraction of pollen tubes grown under the same conditions. (D) Analysis by immunoblotting with antibody to sucrose synthase in the same protein samples described above: cytosol (left), cell wall (centre) and membrane fraction (right). (E) Relative quantification of signals after immunoblotting with antibodies to sucrose synthase in the three fractions described above: cytosol (black bars), cell wall (white bars) and membrane fraction (grey bars). S, sucrose; G, glycerol. Measurements are reported as percentages of total signals.

enzyme, which was very abundant in the apical region and relatively less present in the distal regions. Quantitative analysis confirmed the data by highlighting a significant signal in the first 15–20 µm of pollen tubes and a loss of signal in the following areas (black line in the graph of Fig. 8D). On the contrary, localization of sucrose synthase in pollen tubes grown in glycerol-based medium changed radically. While observing a consistent signal in the apex, the most evident change was an intense signal in the distal areas (Fig. 8B, C). In these regions, sucrose synthase was distributed both in the cell edges and within the cytoplasm with a dot-like pattern, suggesting a possible association/accumulation of the enzyme

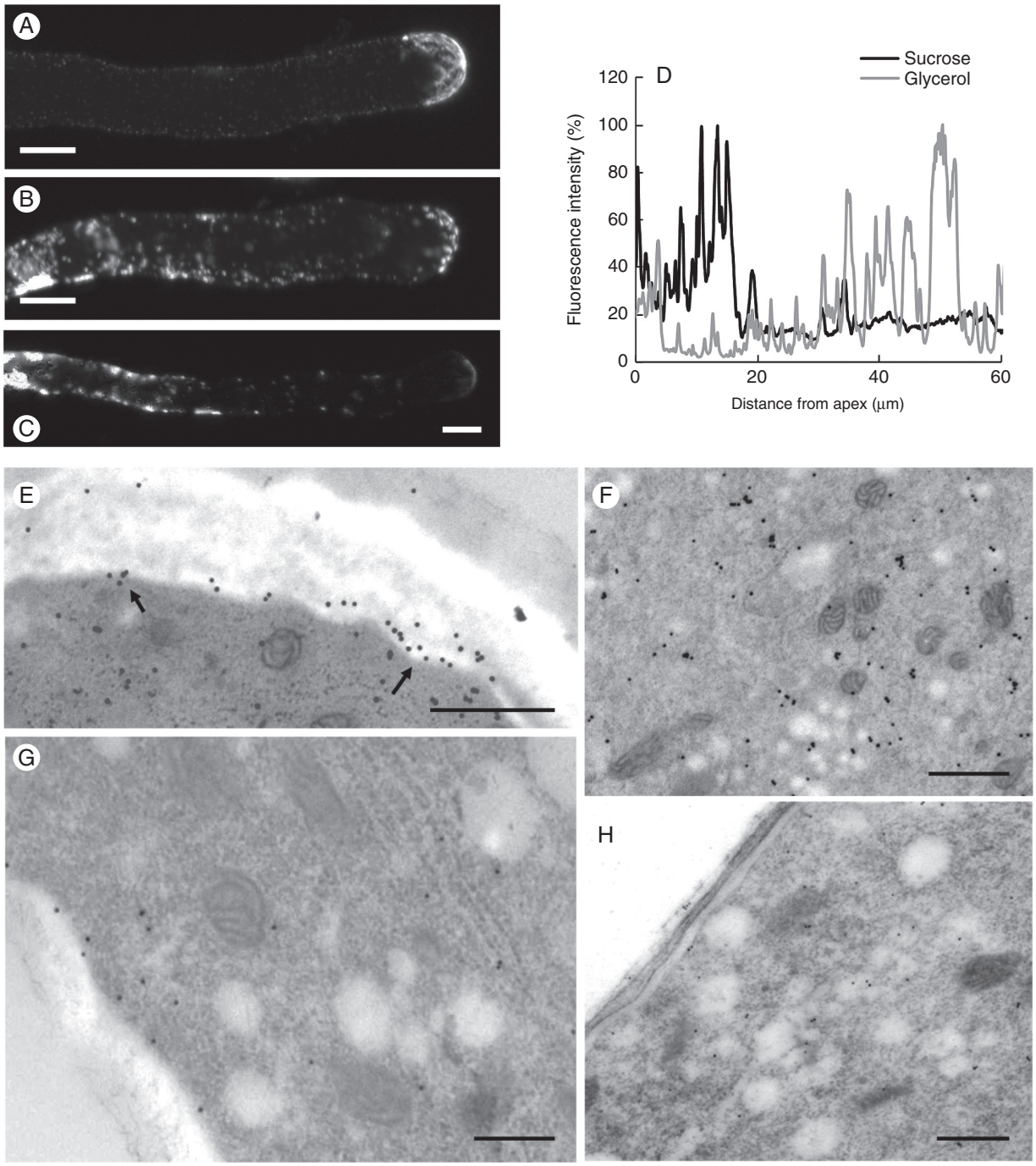

FIG. 8. Distribution of sucrose synthase in pollen tubes grown for 5 h in BKS and BKG. (A) A typical pollen tube labelled with antibody against sucrose synthase. Note the accumulation of signal in the apical region and along the pollen tube edge. Scale bar = 10 μm. (B, C) Two typical pollen tubes grown for 5 h in BKG and labelled with antibody against sucrose synthase. Note the substantial accumulation of signal in distal and internal regions of the tubes. Scale bars = 10 μm. (D) Measurement of sucrose synthase signal along the axis of pollen tubes grown in BKS (black line) and BKG (grey line), starting from the tube apex. (E) Immunogold labelling of sucrose synthase in pollen tubes grown in BKS. In the subapical and distal regions, sucrose synthase is localized in association with the plasma membrane (arrows). Scale bar = 500 nm. (F) The enzyme signal is also found in intracellular membranes. Scale bar = 500 nm. (G) In pollen tubes grown in BKG, the actual amount of sucrose synthase in the subapical region is much smaller and only a few gold particles are observed in association with the plasma membrane. Scale bar = 500 nm. (H) Other subapical sections indicate a very weak signal, suggesting that the amount of sucrose synthase associated with the plasma membrane decreases considerably in BKG. Scale bar = 500 nm.

within cell membranes. This peculiar distribution was particularly evident 40–50 μm from the apex. The different localization was more appreciable after graphical quantitation of the signal (grey line in the graph of Fig. 8D).

Comparative information was also obtained after immunogold labelling with antibody to sucrose synthase. In pollen tubes grown in sucrose-based medium, sucrose synthase was found mainly in association with the plasma membrane

(Fig. 8E, arrows) at the level of the subapical region. In addition to signal associated with the plasma membrane, sucrose synthase was also detected internally, presumably in the cytosol and in association with membranes (Fig. 8F). When pollen tubes were grown in glycerol-based medium, the amount of sucrose synthase in the subapex (as estimated by visual inspection) was very low in comparison with pollen tubes grown in sucrose-based medium (Fig. 8G). Only a few gold particles were observed in association with the plasma membrane. Most of the sections showed a very relative poor signal, indicating that the amount of sucrose synthase in association with the pollen tube plasma membrane decreased considerably (Fig. 8H).

Accumulation and localization of callose synthase are affected by growth media

Callose synthase is involved in the deposition of callose during pollen tube growth. We analysed the accumulation and localization of this enzyme in pollen tubes growing both in the standard condition (with sucrose) and under metabolic stress (with glycerol). We first proceeded with immunoblot analysis to evaluate the quantitative changes in the enzyme during different growth conditions (Fig. 9A). Blot analysis was carried out on protein extracts from membrane compartments of pollen tubes grown for 4, 5 and 6 h in either sucrose- or glycerol-based medium. In the standard condition (with sucrose) we found a higher accumulation of callose synthase at the fourth and fifth hour of growth but a subsequent decrease at the sixth hour of growth (Fig. 9A, blot in bottom panel). This observation was particularly evident and confirmed by measurement and graphing of several blots (Fig. 9B, black bars). In the stressed condition (glycerol medium) we found a different trend of accumulation of callose synthase. Unlike the control condition, we observed a smaller amount of enzyme at the fourth hour then a further decrease at the fifth hour but an increase in accumulation at the sixth hour of growth (Fig. 9A, blot in bottom panel and graph in Fig. 9B, grey bars). In general, the levels of callose synthase in pollen tubes grown in glycerol-based medium were lower than the corresponding controls in sucrose-based medium.

In parallel with the analysis of accumulation, we also tested the localization of callose synthase in pollen tubes grown in different germination media by immunofluorescence microscopy. The analysis was performed only at the fifth hour after germination. In the control, we found that callose synthase was prevalently distributed in the apical region and, to a lesser extent, in more distal parts of the pollen tubes (arrow in Fig. 9C). The inset in Fig 9C (representing a single focal section at the median level of a pollen tube apex) highlights the specific labelling at the level of the apical plasma membrane; this is most likely the cell domain where the enzyme is secreted and inserted. Callose synthase is poorly present in the cell cytoplasm. In pollen tubes grown in the presence of glycerol (Fig. 9D), we identified two substantial changes with respect to standard growing conditions. First, we found a considerable accumulation of the enzyme in the cytoplasm of distal regions; second, we noted a significant reduction in signal at the tube apex. The inset in Fig. 9D shows a distal portion of a pollen tube, in which intracytoplasmic accumulations of callose synthase are evident.

After examining the distribution of callose synthase by immunofluorescence microscopy, we deepened the analysis by using immunoelectron microscopy in the cell areas indicated by the sketches in Fig. 10 (the top sketch refers to BKS analyses, the bottom sketch to BKG analyses). In the apex/subapex region (Fig. 10A), gold particles were found mostly in association with the plasma membrane and in the cell wall. The signal was also evident in association with the vesicular material normally present at the apex of pollen tubes (arrows), suggesting events of exocytosis. In distal regions (Fig. 10B), gold particles were associated with the plasma membrane and sporadically with the inner layer of the cell wall. In the underlying cytoplasm of distal regions, association between callose synthase and microtubular cytoskeleton could be observed. More specifically, gold particles were found in association with longitudinal cortical microtubules (Fig. 10C, arrow), thus suggesting again that microtubules participate in the localization of callose synthase in distal regions.

The distribution of callose synthase was partially different when we analysed pollen tubes grown for 5 h in BKG. First, images at apex/subapex level showed that the amount of enzyme decreased significantly (Fig. 10D). Although the density of gold particles was significantly lower than in the controls, callose synthase was still predominantly associated with the plasma membrane. Another significant difference concerned the distribution of callose synthase in distal regions (Fig. 10E). Here, callose synthase was still found mainly in the plasma membrane and the inner layer of the cell wall. However, a consistent signal was also detected in the cytoplasm of pollen tubes (Fig. 10F), sometimes in association with membrane-like structures, suggesting internalization or lack of secretion of the enzyme.

Distribution of callose changed in pollen tubes grown in different media

The distribution of callose in the subapical region of pollen tubes grown in glycerol-based medium differed in comparison with pollen tubes in standard medium. In pollen tubes grown in sucrose-based medium, the distribution of callose was not significantly different during the transition from 4 to 6 h of germination. In all three cases (4, 5 and 6 h), the relative amount of callose was almost undetectable at the apex, then increased gradually and stabilized at ~15 µm from the apex (Fig. 11A). Distribution of callose was rather different when pollen tubes were grown in glycerol-based medium. After 4 and 6 h of growth, callose was not detected at the very tip region but the aniline blue signal increased rapidly and stabilized around 10–15 µm from the tip. The pattern was different after 5 h of growth because the callose signal was again undetectable at the very tip but increased and stabilized around 20–25 µm from the tip (Fig. 11B). This was not immediately visible after staining with aniline blue (Fig. 11C–E) but became apparent after measurement of callose in different pollen tubes. Consequently, the distribution of callose in 5-h-grown pollen tubes was markedly different from that in both 4- and 6-h-grown pollen tubes.

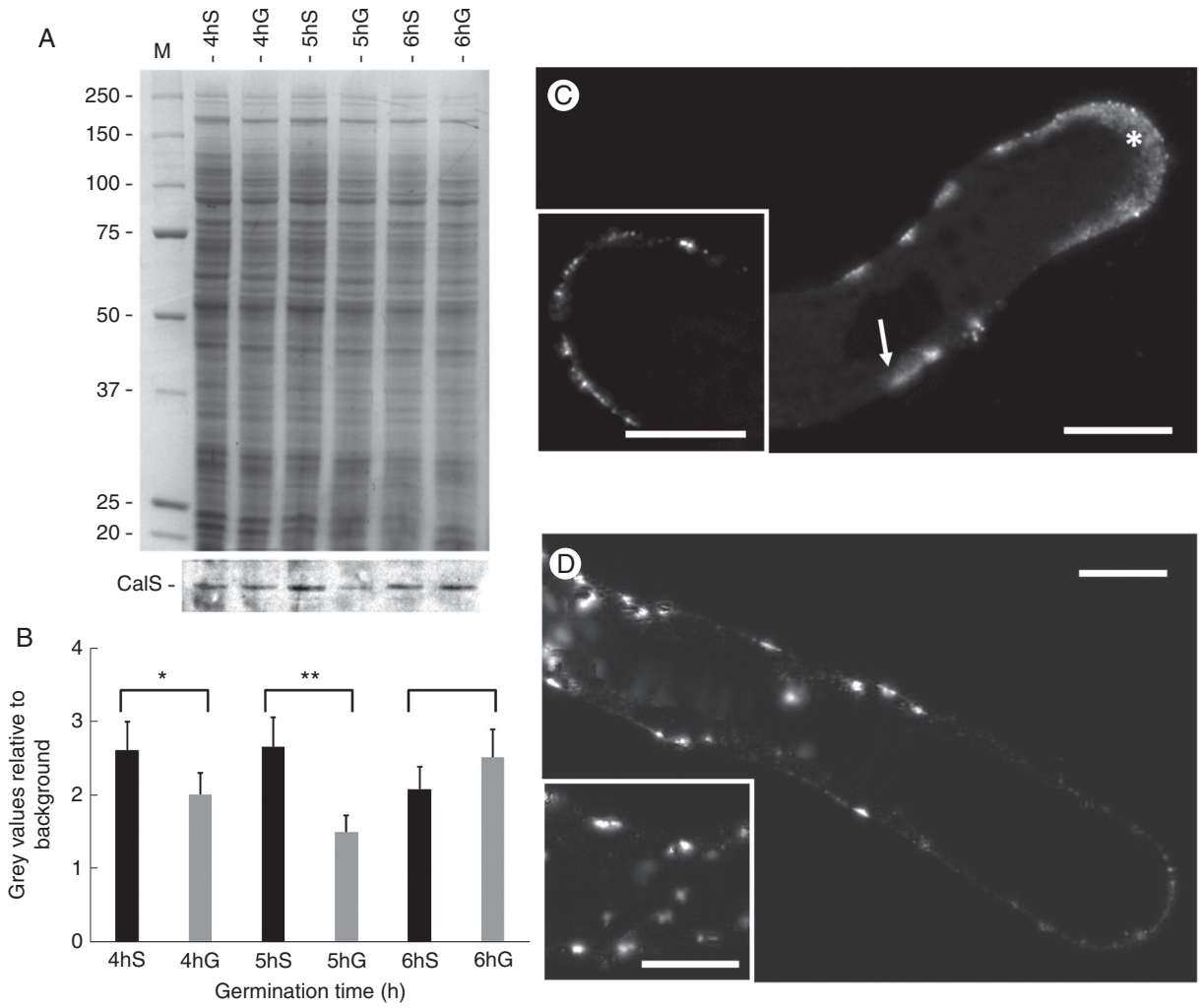

FIG. 9. Analysis of the accumulation and distribution of callose synthase in pollen tubes grown in BKS and BKG for 4, 5 and 6 h. (A) Electrophoresis (top) and immunoblotting (bottom) analysis with antibody to callose synthase (CalS) in different growth conditions. S, sucrose; G, glycerol. (B) Measurement of the immunoblot signal. Black bars, pollen tubes in BKS; grey bars, pollen tubes in BKG. $*P < 0.05$; $**P < 0.01$. (C) Analysis by immunofluorescence microscopy of callose synthase in pollen tubes grown in BKS after 5 h of germination. The enzyme is distributed predominantly in the apical region (asterisk) and, to a lesser extent, in more distal parts of the pollen tubes (arrow). Insert: single focal section approximately at the median level of a pollen tube apex. (D) In pollen tubes grown in BKG, the enzyme accumulates substantially in the cytoplasm of distal regions concomitantly to reduction of signal in the tube apex. Insert: distal portion of a pollen tube with clear intracytoplasmic accumulation of the enzyme. Scale bars = 10 µm.

The composition of growth media affects both generative cell movement and callose plug deposition

An additional feature we evaluated was the relationship between generative cell movement and composition of the growth medium. Using DAPI staining, we analysed the movement of generative cells during growth of pollen tubes in both sucrose- and glycerol-based medium, starting from the third hour of germination. The data are reported as the ratio between the distance covered by generative cells from the grain and the length of corresponding pollen tubes. Data were analysed by two different statistical tests. First, we used ANOVA to prove that some data sets were statistically different. Subsequently, we applied a *t*-test comparative analysis between pairs of data sets obtained in sucrose- and glycerol-based media at the same time of growth. We found that data sets were statistically different only during the fifth hour of growth ($P < 0.05$), as indicated by the asterisk in Fig. 12A. At this specific growth point, the generative cell covered a smaller distance than the controls in sucrose-based medium; in addition, the larger standard deviation suggested a greater range of movement inhomogeneity.

In addition to the measurement of generative cell movement, we also determined the frequency of callose plug deposition after 7 h of growth in both sucrose- and glycerol-based medium. Again, the data were reported as the ratio between the distance of callose plugs (as measured from the grain) and the length of corresponding pollen tubes. In the controls, the first callose plug (the one closest to the grain) was formed with an average ratio of <0.4 while in pollen tubes grown in glycerol-based media the average ratio was around 0.2. On the contrary, the second callose plug (the one closest to the tube apex) was formed in both cases with the same ratio, around 0.6 (Fig. 12B). Apparently, the presence of glycerol-based medium affected the speed of pollen tube elongation during the fourth and fifth hours of growth and, in

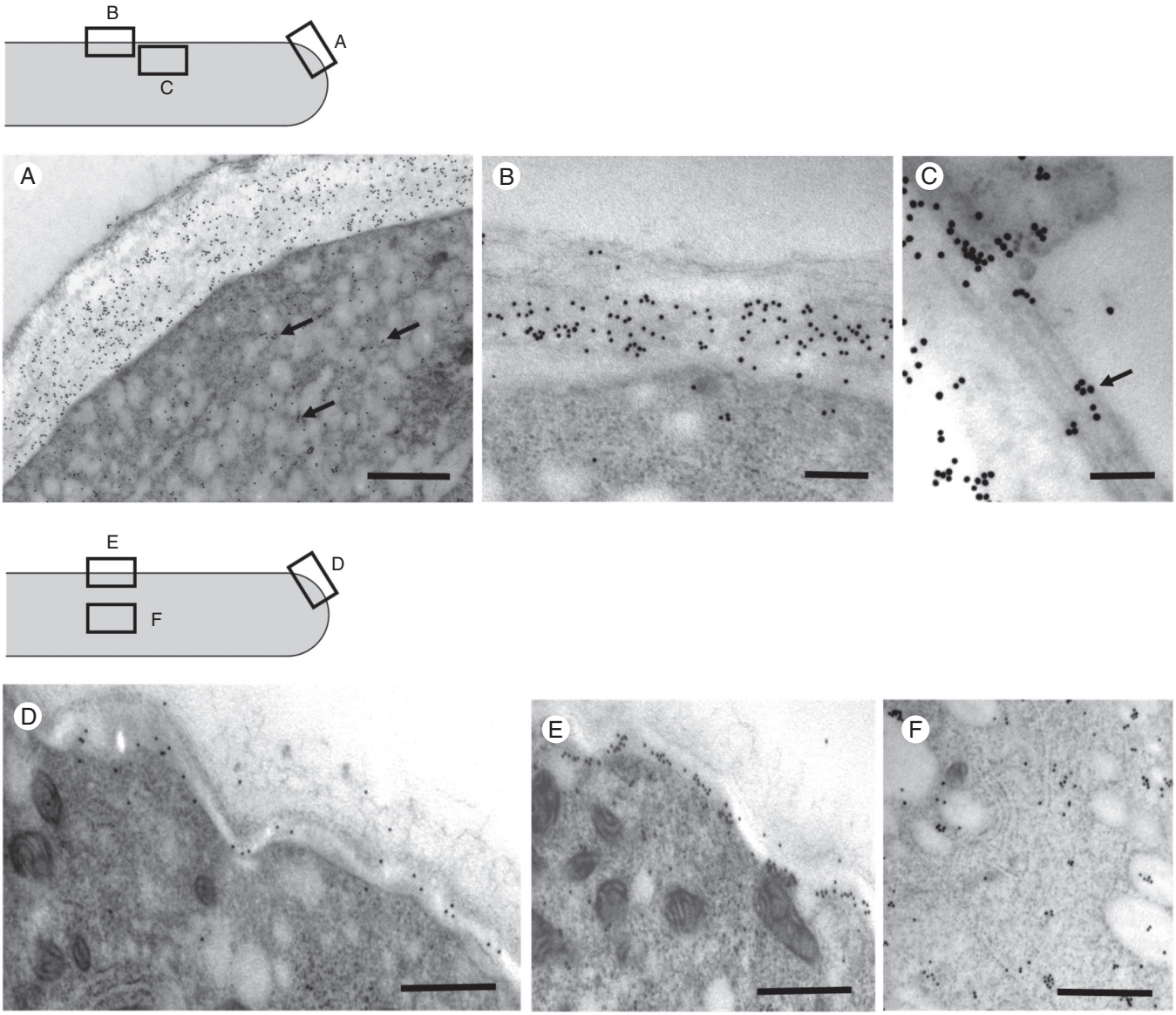

Fig. 10. Analysis of the distribution of callose synthase by immunoelectron microscopy. (A) In the subapical region of pollen tubes grown in sucrose-based medium, callose synthase is strongly detected in association with the plasma membrane and cell wall. The enzyme is also found in association with vesicles in the underlying cytoplasm (arrows). Scale bar = 500 nm. (B) In the most distal regions, the enzyme is still detected in association with the plasma membrane and sporadically with the inner layer of the cell wall. Scale bar = 500 nm. (C) Association between callose synthase and longitudinal cortical microtubules as observed in the underlying cytoplasm (arrow). Scale bar = 150 nm. (D) In pollen tubes grown in glycerol-based medium for 5 h, the amount of enzyme decreases considerably at the apex/subapex level. Scale bar = 500 nm. (E) In the shank region, callose synthase is still predominantly associated with the plasma membrane and the initial layer of the cell wall. Scale bar = 500 nm. (F) Detail of the cytoplasmic region with strong signal of callose synthase. Scale bar = 500 nm.

turn, this determined the early formation of the first callose plug. After 7 h of germination, when the growth rate of pollen tubes was very similar in both experimental conditions, the second callose plug was also formed in the same position relative to pollen tube length. A characteristic and interesting aspect concerned the percentage of deposition of the second callose plug, which, in pollen samples grown in BKG, did not form consistently but at lower percentages (about 32.4 % compared with 63.6 % in pollen tubes grown in BKS). In Fig. 12 panels C and D illustrate, respectively, a representative pollen tube grown for 7 h in BKS (with two callose plugs) and a pollen tube grown in BKG (only the first callose plug is visible).

DISCUSSION

In this article we have analysed the effects of carbon availability on the development of pollen tubes by replacing sucrose with glycerol in the growth medium. Glycerol, unlike sucrose, cannot be efficiently converted into energy. Therefore, when internal stores are depleted, pollen tubes experience an energy deficit. In yeast, glycerol can be used as a carbon source under specific conditions and the catabolic pathway involves phosphorylation by a glycerol kinase and oxidation by a mitochondrial glycerol phosphate-ubiquinone oxidoreductase (Nevoigt and Stahl, 1997). Plant cells can also likely use glycerol as a

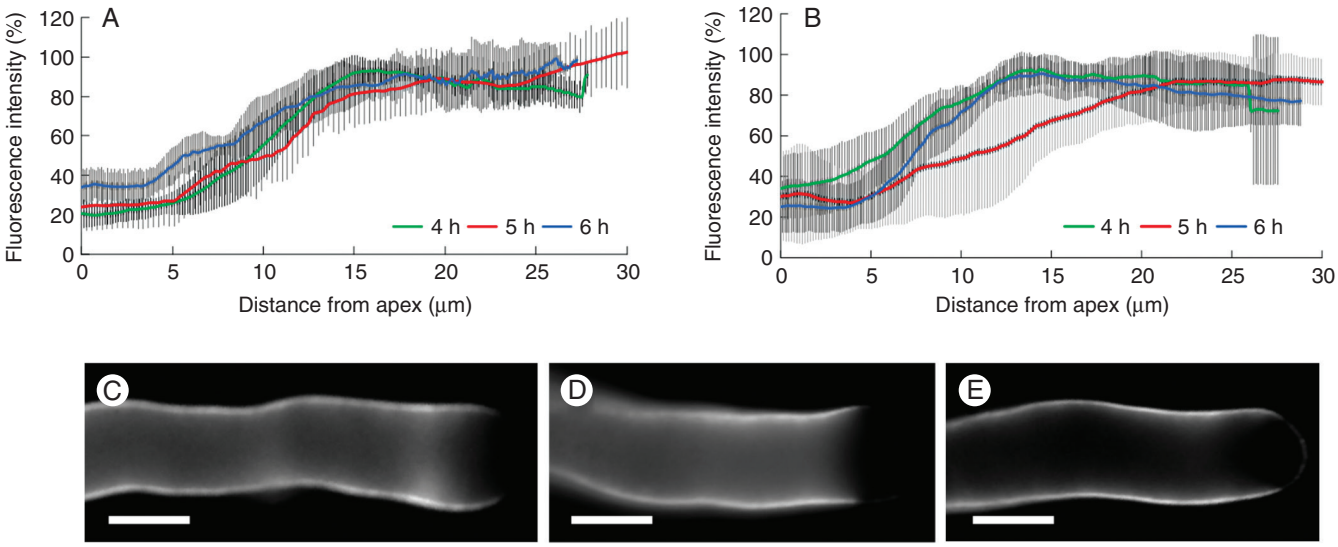

FIG. 11. Distribution of callose in the subapical region of pollen tubes grown in medium with sucrose or glycerol. In all cases, fluorescence was measured starting from the apex down to 30 μm. (A) In medium with sucrose, distribution of callose did not differ during the transition from 4 to 6 h of germination. (B) Distribution of callose differed when pollen tubes were grown in medium with glycerol, especially after 5 h of growth, because the callose signal stabilized only around 20–25 μm from the apex. (C, D, E) Visualization of callose in pollen tubes grown in medium with glycerol, respectively after 4, 5 and 6 h of germination. Scale bars = 10 μm.

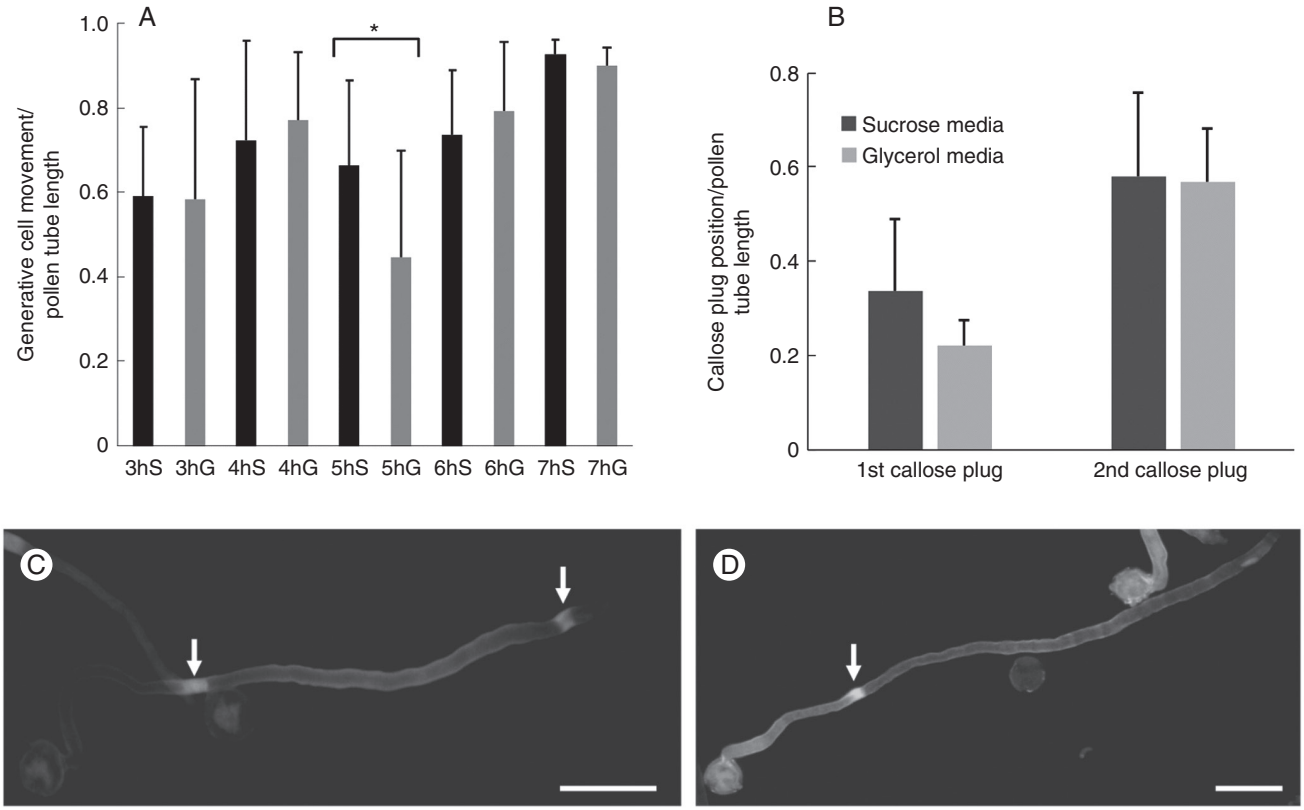

FIG. 12. Effects of germination medium on the translocation of the generative cell and on the deposition of callose plugs. (A) Ratio between the movement of the generative cell from the grain and the corresponding pollen tube length as measured from 3 to 7 h after germination in growth medium containing either sucrose (S, black bars) or glycerol (G, grey bars). Standard deviation is indicated at the top of the bars. *$P < 0.05$. (B) Ratio between positions of the first and second callose plugs and the corresponding pollen tube length as determined after 7 h of germination. The first callose plug is the one closest to the pollen grain. Bars indicate standard deviation. (C) A pollen tube grown in BKS for 7 h, in which two callose plugs (arrows) can be observed. Scale bar = 50 μm. (D) A pollen tube grown for 7 h in BKG containing only the first callose plug (arrow). Scale bar = 50 μm.

carbon source and glycerol-3-phosphate derived from phosphorylation of glycerol is introduced into the glycolic pathway by a cytosolic and/or plastidial NAD-linked glycerol phosphate dehydrogenase. However, high concentrations of glycerol-3-phosphate prevent the flowing back of carbon from triose phosphates to glucose-6-phosphate. This is confirmed by the evidence that glycerol-3-phosphate is a competitive inhibitor of glucose-6-phosphate isomerases and, after sucrose starvation, addition of glycerol to the cell culture does not trigger a rapid accumulation of glucose-6-phosphate in the cytoplasmic compartment and prevents the reloading of intracellular pools of carbohydrates (starch and sucrose) (Aubert *et al.*, 1994). This means that glycerol might enter the metabolism at a later stage and, most likely, it cannot contribute efficiently to the production of UDP-glucose.

As a first analysis, we found that the presence of glycerol substantially changes the length and growth speed of pollen tubes; this is not unexpected because tube growth requires high levels of energy molecules. We monitored the effects of energy deficiency during 6–7 h of growth, during which internal carbohydrate stores would have to be depleted. Surprisingly, the most discernible effect occurred at the fifth hour of growth as a consistent reduction in the growth rate; after that, the growth rate was restored. This specific phase likely corresponds to the depletion of internal energy deposits (autotrophic phase) and the transition to heterotrophic phase, i.e. the consumption of carbohydrates taken up from the extracellular environment. As partial confirmation, low levels of sucrose or starch do not necessarily affect pollen tube growth in tomato, and pollen tubes can apparently use other energy molecules (Garcia *et al.*, 2012).

Pollen tubes might import sugars through two distinct mechanisms. The first involves the cleavage of sucrose by cell wall-associated invertase and the transport of monosaccharides. Glucose and fructose are then readily available in the cytoplasm of pollen tubes (Goetz *et al.*, 2016). This metabolic pathway is probably active when the availability of sucrose is high (i.e. when there is no shortage of carbon). The second import mechanism requires the presence of sucrose transporters, which carry sucrose directly within the cytoplasm (Lemoine *et al.*, 1999; Stadler *et al.*, 1999). According to this alternative metabolic pathway, sucrose can then be used to produce fructose and UDP-glucose by the activity of cytoplasmic sucrose synthase. This second pathway is generally preferred when the availability of carbon is reduced because it saves a greater amount of energy. This could reasonably lead to reduction in the concentration of glucose and fructose in pollen tube cytoplasm because a small amount of fructose would be immediately directed to glycolysis.

The ability of pollen tubes to modify their metabolism under metabolic stress is not surprising because similar effects have already been described when the mitochondrial electron transport chain is blocked by specific inhibitors. In such conditions, pollen tubes exhibit a reduction in growth rate and then switch to fermentative metabolism. Soon after, pollen tubes resume their normal growth rate, suggesting metabolic bypass and plasticity in these cells (Rounds *et al.*, 2010). The metabolic adaptation of pollen is also demonstrated by the rapid changes in the content of metabolites that are observed during the transition from pollen to pollen tube, and even more when the mitochondrial electron transport chain is inhibited (Obermeyer *et al.*, 2013).

The growth of pollen tubes through the style requires considerable amounts of energy. Pollen tubes of lily are estimated to synthesize ~4.4×10^{-14} moles of ATP grain^{-1} s^{-1} during the normal growth process (Rounds *et al.*, 2011*b*). In this study we found a different concentration of ATP between the two growth media. In glycerol-based medium, we found a significant reduction in ATP concentration throughout the analysed period compared with the concentration of ATP in the sucrose-based medium. This could be explained by a different rate of ATP production during metabolic stress, and it is confirmed by the observation that other stresses (such as cold treatment) cause reduction of ATP synthesis in pear pollen tubes (Gao *et al.*, 2014). However, the reduction in ATP synthesis cannot be the only reason for the observed phenomena; in fact, the reduction in ATP concentration is constant throughout the growth period, while most of the effects are observable in a precise time span. Apparently, pollen tubes succeed in balancing the reduced production of ATP to adequately support the growth process.

It is reasonably expected that switching to a different metabolism can affect many collateral processes that directly or indirectly depend on the way energy is produced. In our case, we found significant changes in cell wall structure, such as at the level of pectins. An incorrect deposition of pectins is a characteristic trait after metabolic stress and it may result from either a reduced fusion rate of secretory vesicles at the apex or from a lower content of pectins within vesicles. The synthesis of pectins occurs in the Golgi apparatus and most likely requires the availability of UDP-glucose. A complex metabolic network (Caffall and Mohnen, 2009) is critical for the interconversion of UDP-glucose into energy-rich monosaccharides required for pectin synthesis, such as the conversion of UDP-glucose to UDP-galactose (Huang *et al.*, 2016) and the conversion of UDP-glucose to UDP-glucuronic acid (Klinghammer and Tenhaken, 2007). We suggest that the Golgi-associated sucrose synthase we previously found (Persia *et al.*, 2008) may be important in fuelling the Golgi-bound UDP-glucose transporters (Munoz *et al.*, 1996). Therefore, an altered activity/distribution of sucrose synthase can affect pectin synthesis by reducing the levels of UDP-glucose within Golgi membranes.

The suggested modification of pectin levels is also accompanied by an altered distribution of pectins. Labelling with both PI and, more specifically, JIM7 antibody has shown that pollen tubes grown in BKG have a different, more homogeneous distribution of methyl-esterified pectins than the controls. In parallel and to support this, the profile of acidic pectins also changes. Although the latter are always distributed with regular periodicity, they accumulate at the apex, their levels along the pollen tube are more homogeneous and the ring pattern is much less accentuated. Data on pectins indicate a lower rate of secretion of methyl-esterified pectins, which results in higher levels of acidic pectin at the apex and more homogeneity along tubes. This new distribution pattern mirrors the new type of pollen tube growth, which is more continuous and not oscillatory. Such growth usually occurs when pollen tubes have a more homogeneous cell wall composition (Kroeger *et al.*, 2011).

The differential type of growth (continuous versus oscillatory) was observed both when the growth rate was similar to controls and when it decreased drastically. Therefore, continuous growth is not directly related to different growth rates, but is characteristic of pollen tubes that grow with low carbon

availability. Because the growth of pollen tubes depends on the relationship between turgor pressure and cell wall stiffness, one of the two factors is responsible for the different growth type. If turgor pressure does not change, the new growth medium likely affects cell wall composition. The literature documents changes in the expression of genes coding for cell wall enzymes of pollen tubes growing in different growth media (different sucrose concentrations), indicating that the composition of the germination medium affects the cell wall structure (da Costa *et al.*, 2013). Even a different osmolarity of the growth medium can have effects on the wall composition, as observed when pollen tubes are grown in low-osmolarity media (Biagini *et al.*, 2014).

The lack of standard (oscillatory) growth has already been reported during other stressful conditions, such as in the case of tobacco pollen tubes subjected to heat stress (Parrotta *et al.*, 2015) or when pollen tubes grow in hypotonic media (osmotic stress) (Biagini *et al.*, 2014). However, there are some exceptions. For example, when the electron transport chain is inhibited in lily pollen tubes, the growth of pollen tubes stops temporarily before resuming (as also in our study), but it continues to oscillate (Rounds *et al.*, 2010). Data on lily pollen tubes suggest that oscillatory growth is not directly related to the type of metabolism. In our case, we can assume that the loss of oscillatory growth depends on the amount of energy that pollen tubes take up externally and on the direction of energy flow. Because glycerol may feed glycolysis but not UDP-glucose synthesis, sucrose depletion modifies the way the apical cell wall is assembled.

The current data confirm the results of Persia *et al.* (2008) indicating that pollen tubes grown in glycerol-based medium for 3 h show both a different distribution of sucrose synthase and a deficit of growth, and suggest again that the external availability of sucrose can affect the distribution (and perhaps the activity) of sucrose synthase. In fact, we observed that a scarcity of sucrose causes a lower accumulation of sucrose synthase in the membrane protein fraction as well as in the cell wall protein fraction. In support of this observation, a differential distribution of sucrose synthase in cotton has been proposed in relation to the different use of sucrose. Plausibly, when plant cells need to elongate, sucrose is necessary to fuel the synthesis of cellulose and sucrose synthase is therefore mainly associated with the plasma membrane; when, instead, plant cells suffer sucrose shortage, they need to save energy and sucrose synthase is therefore in the cytosolic form (Haigler *et al.*, 2001). In our case, when pollen tubes are grown in glycerol-based medium, sucrose synthase is likely to accumulate in the cytosol and only part of it moves to the apical plasma membrane or cell wall, perhaps accumulating in intracellular membranes. This redistribution could affect the ability to adequately support the synthesis of cellulose and callose through production of UDP-glucose, thereby affecting cell wall assembly. Although the association between sucrose synthase and cellulose synthase or callose synthase has not yet been established precisely, some work suggests this possibility (Fujii *et al.*, 2010; Brill *et al.*, 2011). Accordingly, the slight but significant changes in the deposition of callose, as observed after 5 h of growth in glycerol-based medium, are not unexpected because the less energetic contribution of glycerol may affect the synthesis of callose.

Changes in callose deposition have a counterpart in the altered distribution of callose synthase. During the fifth hour of growth the content of callose synthase in the membrane fraction decreased significantly. In addition, we observed a significantly lower accumulation of callose synthase in the apical region that resulted in intracellular accumulation. In contrast, during the fourth and sixth hours of growth, the content of callose synthase in the membrane fraction was comparable to controls. At the cytological level, the distribution of the enzymes was also comparable to that described in the literature (Cai *et al.*, 2011). These observations indicate that the transition between the use of internal stores and the consumption of glycerol also affects the distribution of callose synthase. Since the insertion and removal of callose synthase from the plasma membrane is closely related to the vesicular flow (Brownfield *et al.*, 2008), changes in exocytosis/endocytosis may alter the enzyme levels in the apical plasma membrane. It should be noted that similar effects have also been obtained after treatment of tobacco pollen tubes with brefeldin A, a vesicle trafficking inhibitor (Cai *et al.*, 2011). Reduced levels of callose synthase in the apical plasma membrane and its accumulation in the cytoplasm are also supported by immunoelectron microscopy analysis. Therefore, the combination of lower levels of UDP-glucose with incorrect distribution of callose synthase could reasonably determine an altered deposition of callose at the fifth hour of growth. Since callose levels and distribution of callose synthase are re-established during the sixth hour of growth, pollen tubes must necessarily have put in place mechanisms of recovery of callose synthesis in the presence of reduced levels of UDP-glucose.

Other significant effects were observed on proton levels (i.e. intracellular pH values) and ROS. Since the correct distribution of both H^+ and ROS contributes to regulation of the growth of pollen tubes, their anomalous redistribution can be linked to the new type of growth. In pollen tubes, H^+-ATPases are the primary pump responsible for creating proton gradients that are used for myriad active transport processes (such as sucrose transport). These enzymes are also likely important for maintaining a correct pH at the pollen tube tip (Feijò *et al.*, 1999). The pH homeostasis probably depends on the influx of H^+ at the apex and efflux of H^+ as achieved by membrane ATPases (the so-called alkaline band) (Feijò *et al.*, 1999). We found that tobacco pollen tubes grown in sucrose-based media are characterized by an apical acid region, followed by a decrease in proton concentration. Conversely, when pollen tubes are grown in glycerol-based medium, proton levels are more homogeneous. Studies on lily pollen tubes during normal oscillatory growth have revealed that both the acidic tip and the alkaline band oscillate with the same growth period (Lovy-Wheeler *et al.*, 2006). Because in our experiment we observed disappearance of oscillatory growth, this reasonably relates to disappearance of the proton gradient.

Reactive oxygen species are an inevitable consequence of aerobic metabolism but are also produced in a controlled manner and used for a variety of functions, including defence against pathogens and cell signalling (Mittler *et al.*, 2011). In our work, we determined that pollen tubes grown in standard media are characterized by a relatively higher concentration of ROS in the apical region. However, when pollen tubes are grown in glycerol-based medium, ROS show a uniform distribution along the growth axis. In pollen tubes, the presence of ROS is correlated to the calcium gradient since ROS most

likely act as positive feedback for the accumulation of calcium ions, probably by modulating the opening of Ca^{2+} channels at the tube apex (Potocky *et al.*, 2012; Kaya *et al.*, 2014; Lassig *et al.*, 2014; Aloisi *et al.*, 2017). It has also been reported that the synthesis of ROS through NAPDH oxidase is activated by Ca^{2+}, thus forming a positive feedback circuit that reinforces the tip polarity (Potocky *et al.*, 2007). Although a link between the different processes is not immediately clear, it is possible to trace a metabolic pattern from the entrance of energy molecules (sucrose or glycerol) to the effects on pollen tube growth (Fig. 13). The thickness of the arrows in Fig. 13 indicates the hypothetical intensity of each process.

A striking effect after growing pollen tubes in BKG was the change in the deposition of callose plugs. The first callose plug is deposited in advance of the control, while the second plug is deposited as in the controls. The low growth rate observed after glycerol treatment has therefore substantial effects on the deposition of callose plugs, as confirmed by the fact that glycerol treatment does not allow an adequate synthesis of UDP-glucose, the substrate for callose synthesis. The reduction in growth rate is also accompanied by a significant reduction in the movement of generative cells, so much so that the two events could be linked. If the first callose plug is properly deposited during growth in BKG, this could lead to the isolation of generative cells (if they move at slower speeds). Therefore, incorrect deposition of the first callose plug could be interpreted as an attempt not to isolate the generative cell. When the growth of pollen tubes resumes at a speed like that occurring in controls, the second callose plug is deposited in a way comparable to that in controls. This suggests the presence of a link between the growth of pollen tubes, the deposition of callose plugs and the movement of generative cells. Few works in the literature suggest such a relationship; in particular, microtubules have been indicated as connectors between

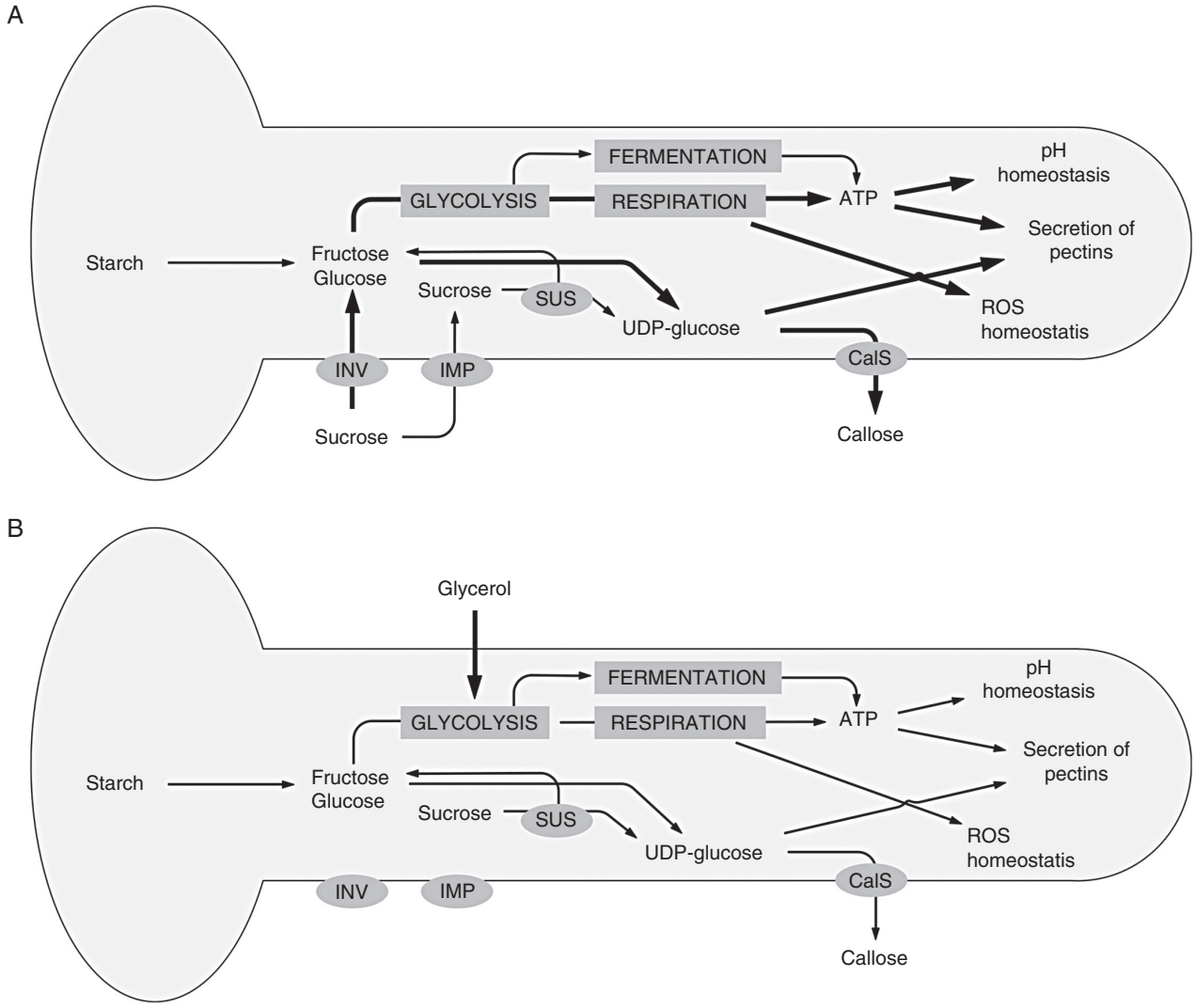

FIG. 13. Schematic illustration of the main metabolic pathways occurring in pollen tubes grown in either sucrose or glycerol. (A) When the growth medium contains sucrose, it feeds glycolysis (and thus respiration) and UDP-glucose synthesis. This provides a normal growth process. (B) When the growth medium contains glycerol, synthesis of UDP-glucose is likely to be reduced; ATP levels are also lower, and this affects the several processes analysed, such as the homeostasis of pH and ROS, and production/secretion of pectins. The growth process is thus altered. The thickness of the arrows indicates the hypothetical intensity of each individual process. CalS, callose synthase; IMP, importer; INV, invertase; SUS, sucrose synthase.

the two processes (Laitiainen *et al.*, 2002). In the present work we did not analyse the organization of microtubules following metabolic stress. We obtained some preliminary indications in actin filaments, which, in pollen tubes grown in BKG, seemed to be organized exactly as in the BKS controls (data not shown). Monitoring the cytoskeleton of pollen tubes in glycerol-based medium could be an interesting research topic to focus on later.

ACKNOWLEDGEMENTS

We are grateful to Mr Massimo Guarnieri (Department of Life Sciences, University of Siena) for technical assistance during HPLC analyses; we also thank the employees of the Botanical Garden of the University of Siena for kindly supporting us and for growing tobacco plants. This work was supported by PRIN 2015 ISIDE (Investigating Self Incompatibility Determinants in fruit trees) (http://prin.miur.it/) to S.D.D. and G.C.

Conflict of Interest: All authors of the manuscript declare that they have no potential sources or conflict/financial interest. The research involves neither human participants nor animals.

LITERATURE CITED

Aloisi I, **Cai G**, **Tumiatti V**, **Minarini A**, **Del Duca SD. 2015**. Natural polyamines and synthetic analogues modify the growth and the morphology of *Pyrus communis* pollen tubes affecting ROS levels and causing cell death. *Plant Science* **239**: 92–105.

Aloisi I, **Cai G**, **Faleri C**, **Navazio L**, **Serafini-Fracassini D**, **Del Duca S. 2017**. Spermine regulates pollen tube growth by modulating Ca^{2+}-dependent actin organization and cell wall structure. *Frontiers in Plant Science* **8**: 1701.

Aubert S, **Gout E**, **Bligny R**, **Douce R. 1994**. Multiple effects of glycerol on plant cell metabolism. Phosphorus-31 nuclear magnetic resonance studies. *Journal of Biological Chemistry* **269**: 21420–21427.

Biagini G, **Faleri C**, **Cresti M**, **Cai G. 2014**. Sucrose concentration in the growth medium affects the cell wall composition of tobacco pollen tubes. *Plant Reproduction* **27**: 129–144.

Brewbaker JL, **Kwack BH. 1963**. The essential role of calcium ion in pollen germination and pollen tube growth. *American Journal of Botany* **50**: 859–865.

Brill E, **van Thournout M**, **White RG**, ***et al.* 2011**. A novel isoform of sucrose synthase is targeted to the cell wall during secondary cell wall synthesis in cotton fiber. *Plant Physiology* **157**: 40–54.

Brownfield L, **Wilson S**, **Newbigin E**, **Bacic A**, **Read S. 2008**. Molecular control of the glucan synthase-like protein NaGSL1 and callose synthesis during growth of *Nicotiana alata* pollen tubes. *Biochemical Journal* **414**: 43–52.

Caffall KH, **Mohnen D. 2009**. The structure, function, and biosynthesis of plant cell wall pectic polysaccharides. *Carbohydrate Research* **344**: 1879–1900.

Cai G, **Romagnoli S**, **Moscatelli A**, ***et al.* 2000**. Identification and characterization of a novel microtubule-based motor associated with membranous organelles in tobacco pollen tubes. *Plant Cell* **12**: 1719–1736.

Cai G, **Faleri C**, **Del Casino C**, **Emons AMC**, **Cresti M. 2011**. Distribution of callose synthase, cellulose synthase and sucrose synthase in tobacco pollen tube is controlled in dissimilar ways by actin filaments and microtubules. *Plant Physiology* **155**: 1169–1190.

Cai G, **Parrotta L**, **Cresti M. 2015**. Organelle trafficking, the cytoskeleton, and pollen tube growth. *Journal of Integrative Plant Biology* **57**: 63–78.

Certal AC, **Almeida RB**, **Carvalho LM**, ***et al.* 2008**. Exclusion of a proton ATPase from the apical membrane is associated with cell polarity and tip growth in *Nicotiana tabacum* pollen tubes. *Plant Cell* **20**: 614–634.

Chen CY, **Wong EI**, **Vidali L**, ***et al.* 2002**. The regulation of actin organization by actin-depolymerizing factor in elongating pollen tubes. *Plant Cell* **14**: 2175–2190.

da Costa ML, **Pereira LG**, **Coimbra S. 2013**. Growth media induces variation in cell wall associated gene expression in *Arabidopsis thaliana* pollen tube. *Plants* **2**: 429–440.

Feijò JA, **Sainhas J**, **Hackett GR**, **Kunkel JG**, **Hepler PK. 1999**. Growing pollen tubes possess a constitutive alkaline band in the clear zone and a growth-dependent acidic tip. *Journal of Cell Biology* **144**: 483–496.

Fricker MD, **White NS**, **Obermeyer G. 1997**. pH gradients are not associated with tip growth in pollen tubes of *Lilium longiflorum*. *Journal of Cell Science* **110**: 1729–1740.

Fujii S, **Hayashi T**, **Mizuno K. 2010**. Sucrose synthase is an integral component of the cellulose synthesis machinery. *Plant and Cell Physiology* **51**: 294–301.

Gao YB, **Wang CL**, **Wu JY**, ***et al.* 2014**. Low temperature inhibits pollen tube growth by disruption of both tip-localized reactive oxygen species and endocytosis in *Pyrus bretschneideri* Rehd. *Plant Physiology and Biochemistry* **74**: 255–262.

Garcia CC, **Guarnieri M**, **Pacini E. 2012**. Tomato pollen tube development and carbohydrate fluctuations in the autotrophic phase of growth. *Acta Physiologiae Plantarum* **34**: 2341–2347.

Goetz M, **Guivarc'h A**, **Hirsche J**, ***et al.* 2016**. Metabolic control of tobacco pollination by sugars and invertases. *Plant Physiology* **173**: 984–997.

Gu F, **Nielsen E. 2013**. Targeting and regulation of cell wall synthesis during tip growth in plants. *Journal of Integrative Plant Biology* **55**: 835–846.

Haigler CH, **Ivanova-Datcheva M**, **Hogan PS**, ***et al.* 2001**. Carbon partitioning to cellulose synthesis. *Plant Molecular Biology* **47**: 29–51.

Heinlein M, **Starlinger P. 1989**. Tissue- and cell-specific expression of the two sucrose synthase isoenzymes in developing maize kernels. *Molecular and General Genetics* **215**: 441–446.

Hirose T, **Zhang Z**, **Miyao A**, **Hirochika H**, **Ohsugi R**, **Terao T. 2010**. Disruption of a gene for rice sucrose transporter, OsSUT1, impairs pollen function but pollen maturation is unaffected. *Journal of Experimental Botany* **61**: 3639–3646.

Huang JH, **Kortstee A**, **Dees DCT**, **Trindade LM**, **Schols HA**, **Gruppen H. 2016**. Alteration of cell wall polysaccharides through transgenic expression of UDP-Glc 4-epimerase-encoding genes in potato tubers. *Carbohydrate Polymers* **146**: 337–344.

Kaya H, **Nakajima R**, **Iwano M**, ***et al.* 2014**. Ca^{2+}-activated reactive oxygen species production by *Arabidopsis* RbohH and RbohJ is essential for proper pollen tube tip growth. *Plant Cell* **26**: 1069–1080.

Klinghammer M, **Tenhaken R. 2007**. Genome-wide analysis of the UDP-glucose dehydrogenase gene family in *Arabidopsis*, a key enzyme for matrix polysaccharides in cell walls. *Journal of Experimental Botany* **58**: 3609–3621.

Kroeger JH, **Zerzour R**, **Geitmann A. 2011**. Regulator or driving force? The role of turgor pressure in oscillatory plant cell growth. *PLoS One* **6**: e18549.

Laemmli UK. 1970. Cleavage of structural proteins during the assembly of the head of bacteriophage T4. *Nature* **227**: 680–685.

Laitiainen E, **Nieminen KM**, **Vihinen H**, **Raudaskoski M. 2002**. Movement of generative cell and vegetative nucleus in tobacco pollen tubes is dependent on microtubule cytoskeleton but independent of the synthesis of callose plugs. *Sexual Plant Reproduction* **15**: 195–204.

Lang V, **Pertl-Obermeyer H**, **Safiarian MJ**, **Obermeyer G. 2014**. Pump up the volume – a central role for the plasma membrane H(+) pump in pollen germination and tube growth. *Protoplasma* **251**: 477–488.

Lassig R, **Gutermuth T**, **Bey TD**, **Konrad KR**, **Romeis T. 2014**. Pollen tube NAD(P)H oxidases act as a speed control to dampen growth rate oscillations during polarized cell growth. *Plant Journal* **78**: 94–106.

Lemoine R, **Burkle L**, **Barker L**, **Sakr S**, ***et al.* 1999**. Identification of a pollen-specific sucrose transporter-like protein NtSUT3 from tobacco. *FEBS Letters* **454**: 325–330.

Li YQ, **Faleri C**, **Geitmann A**, **Zhang HQ**, **Cresti M. 1995**. Immunogold localization of arabinogalactan proteins, unesterified and esterified pectins in pollen grains and pollen tubes of *Nicotiana tabacum* L. *Protoplasma* **189**: 26–36.

Li YQ, **Mareck A**, **Faleri C**, **Moscatelli A**, **Liu Q**, **Cresti M. 2002**. Detection and localization of pectin methylesterase isoforms in pollen tubes of *Nicotiana tabacum* L. *Planta* **214**: 734–740.

Liu H, **Jiang Y**, **Luo Y**, **Jiang W. 2006**. A simple and rapid determination of ATP, ADP and AMP concentrations in pericarp tissue of litchi fruit by high performance liquid chromatography. *Food Technology and Biotechnology* **44**: 531–534.

Lovy-Wheeler A, **Kunkel JG**, **Allwood EG**, **Hussey PJ**, **Hepler PK. 2006**. Oscillatory increases in alkalinity anticipate growth and may regulate actin dynamics in pollen tubes of lily. *Plant Cell* **18**: 2182–2193.

Malho R, **Liu Q**, **Monteiro D**, **Rato C**, **Camacho L**, **Dinis A. 2006**. Signalling pathways in pollen germination and tube growth. *Protoplasma* **228**: 21–30.

Mellema S, **Eichenberger W**, **Rawyler A**, **Suter M**, **Tadege M**, **Kuhlemeier C. 2002**. The ethanolic fermentation pathway supports respiration and lipid biosynthesis in tobacco pollen. *Plant Journal* **30**: 329–336.

Mittler R, **Vanderauwera S**, **Suzuki N**, ***et al.*** **2011**. ROS signaling: the new wave? *Trends in Plant Science* **16**: 300–309.

Munoz P, **Norambuena L**, **Orellana A. 1996**. Evidence for a UDP-glucose transporter in Golgi apparatus-derived vesicles from pea and its possible role in polysaccharide biosynthesis. *Plant Physiology* **112**: 1585–1594.

Nashilevitz S, **Melamed-Bessudo C**, **Aharoni A**, **Kossmann J**, **Wolf S**, **Levy AA. 2009**. The legwd mutant uncovers the role of starch phosphorylation in pollen development and germination in tomato. *Plant Journal* **57**: 1–13.

Nevoigt E, **Stahl U. 1997**. Osmoregulation and glycerol metabolism in the yeast *Saccharomyces cerevisiae*. *FEMS Microbiology Reviews* **21**: 231–241.

Obermeyer G, **Fragner L**, **Lang V**, **Weckwerth W. 2013**. Dynamic adaption of metabolic pathways during germination and growth of lily pollen tubes after inhibition of the electron transport chain. *Plant Physiology* **162**: 1822–1833.

Parrotta L, **Faleri C**, **Cresti M**, **Cai G. 2015**. Heat stress affects the cytoskeleton and the delivery of sucrose synthase in tobacco pollen tubes. *Planta* **243**: 43–63.

Persia D, **Cai G**, **Del CC**, **Faleri C**, **Willemse MT**, **Cresti M. 2008**. Sucrose synthase is associated with the cell wall of tobacco pollen tubes. *Plant Physiology* **147**: 1603–1618.

Pertl H, **Pockl M**, **Blaschke C**, **Obermeyer G. 2010**. Osmoregulation in *Lilium* pollen grains occurs via modulation of the plasma membrane H+ATPase activity by 14-3-3 proteins. *Plant Physiology* **154**: 1921–1928.

Potocky M, **Jones MA**, **Bezvoda R**, **Smirnoff N**, **Zarsky V. 2007**. Reactive oxygen species produced by NADPH oxidase are involved in pollen tube growth. *New Phytologist* **174**: 742–751.

Potocky M, **Pejchar P**, **Gutkowska M**, ***et al.*** **2012**. NADPH oxidase activity in pollen tubes is affected by calcium ions, signaling phospholipids and Rac/Rop GTPases. *Journal of Plant Physiology* **169**: 1654–1663.

Reinders A. 2016. Fuel for the road – sugar transport and pollen tube growth. *Journal of Experimental Botany* **67**: 2121–2123.

Rodriguez-Garcia MI, **M'rani-Alaoui M**, **Fernandez MC. 2003**. Behavior of storage lipids during development and germination of olive (*Olea europaea* L.) pollen. *Protoplasma* **221**: 237–244.

Rounds CM, **Hepler PK**, **Fuller SJ**, **Winship LJ. 2010**. Oscillatory growth in lily pollen tubes does not require aerobic energy metabolism. *Plant Physiology* **152**: 736–746.

Rounds CM, **Lubeck E**, **Hepler PK**, **Winship LJ. 2011*a***. Propidium iodide competes with Ca(2+) to label pectin in pollen tubes and *Arabidopsis* root hairs. *Plant Physiology* **157**: 175–187.

Rounds CM, **Winship LJ**, **Hepler PK. 2011*b***. Pollen tube energetics: respiration, fermentation and the race to the ovule. *AoB Plants* **2011**: lr019.

Selinski J, **Scheibe R. 2014**. Pollen tube growth: where does the energy come from? *Plant Signaling and Behaviour* 9: e977200.

Smirnova AV, **Matveyeva NP**, **Yermakov IP. 2014**. Reactive oxygen species are involved in regulation of pollen wall cytomechanics. *Plant Biology* **16**: 252–257.

Speranza A, **Crinelli R**, **Scoccianti V**, **Geitmann A. 2012**. Reactive oxygen species are involved in pollen tube initiation in kiwifruit. *Plant Biology* **14**: 64–76.

Stadler R, **Truernit E**, **Gahrtz M**, **Sauer N. 1999**. The AtSUC1 sucrose carrier may represent the osmotic driving force for anther dehiscence and pollen tube growth in *Arabidopsis*. *Plant Journal* **19**: 269–278.

Wang L, **Wang W**, **Wang YQ**, ***et al.*** **2013**. *Arabidopsis* galacturonosyltransferase (GAUT) 13 and GAUT14 have redundant functions in pollen tube growth. *Molecular Plant* **6**: 1131–1148.

Williams JH. 2008. Novelties of the flowering plant pollen tube underlie diversification of a key life history stage. *Proceedings of the National Academy of Sciences of the USA* **105**: 11259–11263.

Winship LJ, **Obermeyer G**, **Geitmann A**, **Hepler PK. 2011**. Pollen tubes and the physical world. *Trends in Plant Science* **16**: 353–355.

Winship LJ, **Rounds C**, **Hepler KP. 2017**. Perturbation analysis of calcium, alkalinity and secretion during growth of lily pollen tubes. *Plants* **6**: 3.

Zerzour R, **Kroeger J**, **Geitmann A. 2009**. Polar growth in pollen tubes is associated with spatially confined dynamic changes in cell mechanical properties. *Developmental Biology* **334**: 437–446.

Zienkiewicz A, **Zienkiewicz K**, **Rejon JD**, **Rodriguez-Garcia MI**, **Castro AJ. 2013**. New insights into the early steps of oil body mobilization during pollen germination. *Journal of Experimental Botany* **64**: 293–302.